ULTRASONIC THERMOMETRY FOR LMFBR SYSTEMS

Phase I Report

Contract No. AT(30-1)-3906

Prepared by

S. S. Fam, L. C. Lynnworth and E. H. Carnevale

September 1968

Work performed for

Development Contracts Division
U. S. Atomic Energy Commission
New York Operations Office
New York, New York

by

DISTRIBUTION OF THIS DOCUMENT IS UNLIMITED

DISCLAIMER

DISCLAIMER

Portions of this document may be illegible in electronic image products. Images are produced from the best available original document.

ULTRASONIC THERMOMETRY FOR LMFBR SYSTEMS

by

S. S. Fam, L. C. Lynnworthand E. H. Carnevale

ABSTRACT

A pulse-echo ultrasonic thermometer system for the development and operation of advanced liquid metal fast breeder reactors (LMFBR) was designed, constructed and tested. The thermometer was designed to determine fuel temperature up to 5000^oF and the coolant and cladding temperatures up to $\sim 1200^o$F by measuring the round trip transit time in wire or tubular sensors. A new instrument was used to measure transit time automatically. Compatibility of the ultrasonic transmission line portion of the system with liquid sodium was demonstrated by immersing bare and sheathed wires up to 20 ft long in sodium up to 700^oF, the maximum temperature attainable in the facility available for this test. The feasibilities of using the spacer wire to measure coolant temperature, and the cladding to measure its own temperature, were also demonstrated. Low frequency mechanical vibrations were shown not to noticeably affect the transit time measurements. Finally, a complete system was simulated in parts, demonstrating that pulses generated in a 100 psi pressure tight magnetostrictive transducer housing could be transmitted down a 50 ft SS 304 lead-in, 'a 20 ft portion of which was sheathed and heated to 1200^oF, with another portion curved into a 2'' radius S-shape simulating access restrictions expected in LMFBR's. With this simulation system echoes were obtained from a 2'' Re sensor at 5000^oF. The ultrasonic instrument automatically measured the time between these echoes to 0.1 psec, corresponding to temperature resolution better than 1% at 5000^oF.

TABLE OF CONTENTS

TABLE OF CONTENTS - CONT'D.

LIST OF FIGURES

LIST OF FIGURES - CONT'D.

V

SUMMARY

The object of this program is to develop an ultrasonic temperature measuring system to automatically determine fuel temperatures up to -5000^oF, and coolant and cladding temperatures up to -1200^oF. The system exploits the temperature dependence of sound velocity in solids and utilizes a pulse-echo technique to measure the round trip transit time in a wire or tubular sensor. This transit time is automatically measured by a new instrument developed in this program.

The sensor materials which yield sufficiently accurate measurements at their respective operating temperatures, are Re for the fuels, and SS 304 for the coolant and cladding. Lead-in wires are of SS 304. The lead-in wires will be placed in protective sheaths, e. g., SS 304. In the reactor core, the rhenium sensor will be placed in a protective sheath which is compatible with the fuel employed. At present, it appears that a Ta or W/Re sheath may be used with UO_2 fuels and W/Re alloys may-be usable in mixed oxide fuels of UO_2 - PuO_2.

Tests performed with empty prototype cladding of the type used in EBR-II fuel demonstrated the feasibility of using the tube itself as an ultrasonic sensor to measure its own average temperature. The effects of the fuel and sodium bond, however, remain to be considered.

Further, the use of the spiral spacing wire as a sensor was also demonstrated. This sensor may measure temperature in sodium external to the cladding.

Attenuation measurements in SS 304 and Re at simulated system operating conditions of geometry and temperature established the minimum signal amplitude required at room temperature from a short attenuation-free line to be on the order of 1 volt.

Electrically heated Re wires were cycled in vacuum to -5000^oF with reproducible results. When heated in UO_2 by the same technique, no observable effect of the UO_2 on the sound velocity in Re was detected up to $\sim 2000^o$F.

Sodium immersion tests at the Argonne National Laboratory, up to the maximum obtainable temperature of the facility, -700^oF, demonstrated that the ultrasonic thermometer can work in molten sodium.

Vibration effects on the signal stability and read-out were investigated and found not to noticeably affect the measurements.

1

Finally, the complete system was successfully tested under simulated conditions pertinent to this application including the following: sensor operating temperatures ranging to -5000° F; lead lengths of 50 ft, 20 ft of which were at temperatures ranging to -1200° F, lead wire transmission through feedthroughs capable of containing vapor pressures of 100 psi, and operation with the lead wire containing bends with 2'' radius of curvature.

The experimental results demonstrate that the goals of Phase I were met. Based on the above, approval was obtained to enter into Phase ll of this program.

The highlights of the **work** performed during Phase I have been reported in a paper to be presented at the 15th Nuclear Science Symposium, Montreal, Canada, October 23-25, 1968[13].

2

INTRODUCTION

Statement of the Problem - Objective

The object of this AEC–sponsored program was to develop an ultra-sonic temperature measuring system for automatically determining the fuel meat, cladding and coolant temperatures in advanced liquid metal cooled fast breeder reactors (LMFBR' s).

Phase I Accomplishments

The nature and scope of the work accomplished in Phase I of this program were as follows.

(i) Conduct high temperature ultrasonic tests to establish velocity/temperature relations and amplitude/temperature relations, necessary for the development of an ultrasonic high temperature measurement system, in materials used in LMFBR cores and'in candidate sensor materials for temperatures ranging up to 5000°F. Materials investi-gated included SS 304, SS 316, Cb, Cb-1% Zr and Re.

(ii) Investigate interactions between the ultrasonic temperature measuring system and materials used in LMFBR' s in various geometrical configurations.

(iii) Design, construct and laboratory test a complete ultra-sonic high temperature measurement system based on above investigations.

Prior to field testing in a selected facility, the ultrasonic thermometer system designed and constructed during this phase of the program was operated under laboratory con-ditions to demonstrate the ability of the system to measure temperatures ranging to 5000°F with a Re sensor. Measurement of pulse transit time with an accuracy of ± 0.1 microsecond was demonstrated. System ability to operate with the sensor, and lead-in in a geometrical configuration similar to that encountered in a fast breeder reactor was also demonstrated, including the following: lead lengths of 50 ft, lead wire transmission through liquid

3

sodium, lead wire transmission through feedthroughs capable of containing vapor pressures of 100 psi, and operation with the lead wire containing bends with a 2" radius of curvature.

Present Ultrasonic Approach

The proposed ultrasonic temperature measuring system for LMFBR's (Figs. 1 and 2) is in some respects similar to that being developed by Panametrics in NASA programs' to measure temperature in a nuclear rocket engine. These systems exploit the temperature dependence of sound velocity in refractory metal wires. The system is basically comprised of four parts: transducer, lead-in, sensor, and an electronic transmitter/receiver and read-out instrument. Additionally, a sheath is often used to protect the sensor and lead-in wires from the hostile environment and to simplify handling and installation. The transducer consists of a coil wound around a suitable magnetostrictive wire (usually a nickel alloy). The coil *is* pulsed, thus producing an elastic strain in the wire. In axially magnetized wires[2] an extensional wave[*] then propagates along the wire, and is reflected and/or transmitted according to the geometry and materials used in the line. The reflected waves will generate a signal upon reaching the coil according to the inverse magnetostrictive effect. Of particular interest are the reflections emanating from the beginning and end of the sensor element, the time interval between which is a measure of its average temperature. The time interval is automatically measured and digitally displayed. Since extensional and torsional waves propagate at speeds proportional to the square root of Young's modulus E and to the modulus of 'rigidity G, respectively, it is necessary to consider all the possible mechanisms by which the environment may affect these moduli, and the density.

Features of Ultrasonics

Compared to alternative temperature-measuring systems, thin wire ultrasonic thermometers offer a number of attractive features. These features include a relatively large latitude in materials selection, and an absence of high temperature electrical insulation (except possibly at the magnetostrictive transducer, where temperatures are not as high as at the sensor itself). The ultrasonic measurement of temperature depends upon the density and the elastic properties of the sensor, not its electrical properties. The ultrasonic sensor consists of a single wire which may be of one material only, such as pure Re, and is therefore not subject to the calibration shifts which, in thermocouples, are due to phenomena such as diffusion of one leg into another.

---

[*] In circumferentially magnetized wires, a torsional wave may be launched by the Wiedemann effect.

4

Further, the small thermal mass* of wire sensors will result in a smaller measurement error due to internal heat generation from, say, gamma radiation.

Another significant feature is the possibility of using, as a sensor, the very component whose temperature is required. This is illustrated in a later section where the feasibility of using the cladding as a sensor is discussed.

BRIEF. REVIEW OF BASIC ACOUSTIC PRINCIPLES

Propagation of Elastic Waves in Solids

The elastic waves of interest in this program are the torsional and the non-dispersive extensional waves which propagate respectively at velocities given by

$$V_T = \sqrt{\frac{G}{\rho}}$$

and

$$V_O = \sqrt{\frac{E}{\rho}}$$

where G and E are the moduli of shear and elasticity and ρ is the density. The ranges of validity of the above equations are readily found in the literature[3].

The application of the present ultrasonic approach to thermometry hinges upon the temperature dependence of the elastic moduli and, to a lesser extent, the density.

The extensional velocity/temperature characteristics for W, Re, Mo, Ta, and SS 304 are shown in Fig. 3.

---

*

  Measurements were recently performed at Panametrics with a 0. 001'' diameter tungsten sensor (McDonough et al, ⁻ unpublished).

Wave Reflection and Transmission

A wave will generally be partially reflected and partially transmitted upon reaching a geometric discontinuity or a boundary between two different media. The amplitudes of the reflected and transmitted waves relative to the incident waves are given by

$$\frac{A_{reflected}}{A_{incident}} = \frac{r-1}{r+1} \tag{3}$$

$$\frac{A_{transmitted}}{A_{incident}} = \frac{2r}{r+1} \tag{4}$$

where

$$r = \frac{Z_2}{Z_1} \tag{5}$$

is the ratio of mechanical impedances at the boundary. Expressions (3), (4), and (5) hold for torsional as well as extensional waves. The mechanical torsional wave impedance is

$$Z_T = \rho V_T J \tag{6}$$

whereas the mechanical extensional wave impedance is

$$Z_O = \rho V_O A \tag{7}$$

where J is the polar moment of inertia and A is the cross-sectional area.

Consider the typical ultrasonic line shown in Fig. 4. Applying equations (3) and (4) one can determine the "echo ratio" defined as the ratio of the amplitude of the pulse reflected off the end of the line to that of the pulse reflected from the mismatched boundary 2-3 ($Z_2 \neq Z_3$). The result is:

$$ER = \frac{4r}{1-r^2} \tag{8}$$

where

$$r = Z_3/Z_2$$

Clearly, the echo ratio may take any value between zero (r = 0) and infinity (r = 1). The value of r may be selected such that the echo ratio at the highest operating temperature is close to unity. This is done primarily in order to compensate for signal attenuation due to high temperatures. Fig. 5 illustrates the echo amplitude for multiple echoes. (See also Appendix I.)

The Sensor

In selecting the appropriate material and geometry for any given application, the following factors should be considered:

a) Materials Compatibility with the Environment

' The environment within the reactor core primarily includes UO_2 or other fuel alloys at temperatures up to $-5000^{o}F$, intense thermal and fast neutron fluxes (-10^{15} n/cm^2 sec, 10^{22} to 10^{23} nvt in one year of continuous operation) and gamma radiation.

The highest temperature requirement clearly precludes the use of all but the five refractory elements Ta, **Os,** Re, W and C, and possibly certain refractory alloys and compounds. In Phase I, attention was focused on Re for the fuel temperature measurement, on *SS* 304 cladding to measure its own temperature, and on the SS 304 spiral spacer wire, to measure coolant temperature next to the fuel pin.

From the standpoint of chemical and metallurgical compatibility, and to avoid damping or false echoes from fuel, *the* present view *is* to place the fuel meat sensor in a protective sheath. The choice of materials and dimensions for the sheath will be largely based upon the latest technological advances in thermocouple sheath development for similar environments; for example, SS sheaths (*e*.g. type 304, or type 12R72HV containing molybdenum and titanium recently developed by Sandvik Steel for canning material in sodium cooled fast reactors*) (to protect the lead-in) up to $-1600^{o}F$ in liquid sodium, Ta or W-Re sheaths in UO_2 fuels, and W-Re-Mo sheaths in mixed oxide UO_2-PuO_2 fuels.

---

*Materials Engineering, Vol. 68, No. 7, Dec. 1968, p. 28.

b) <u>Sensitivity of the Temperature Measurement</u>

In general, the required length of the sensing element is dependent upon the interplay between the desired sensitivity to temperature changes at a given temperature, the time resolution of the supporting equipment, the sensor sound propagation properties as characterized by its $V(T)$ curve and its attenuation as a function of frequency and temperature, and the temperature localization required by geometry or by temperature gradients. (See Appendix I).

<u>LABORATORY TEST PROGRAM - SCOPE AND RESULTS</u>

<u>Attenuation in W, Re, and *SS* 304</u>

To determine the operating frequency for ultrasonic transmission over a 50 ft lead-in wire, sound propagation was measured in W, **Cb,** Cb-1% Zr, Re and SS 304 and 316 up to $\sim 2000^o$F. Tungsten was least attenuating. The transmission characteristics of a 0. 050" dia **x** 50 ft W lead-in wire were studied as a function of frequency. The last 20 ft of the W wire were electrically self-heated to temperatures exceeding 2000^oF (Fig. 6). The temperature was determined by means of a chromel-alumel thermocouple attached to the midpoint of the 20 ft heated length, and cross-checked with the known velocity/ temperature characteristic of tungsten. It was found that a 3" coil excited with a 37 microsecond square voltage pulse yielded signals of sufficient amplitude at the required operating temperatures, while higher frequency pulses on shorter coil lengths were overly attenuated. The oscilloscope displays at 1000^oF and 2066^oF are shown in Figs. 7 and 8. The 1000^oF test was performed using a single 3" coil, a GR model 1217C unit pulser and a GR type 1397A pulse amplifier; the high temperature test was conducted with the addition of two 3" coils for transmission and reception. The attenuation at 1000^oF was < 1db/20 ft while the attenuation at 2066^oF was − 6db/20 ft. Of course, use of long lead-in wires having expansion coefficients different from that of the SS sheath, despite attractively lower attenuation, introduces mechanical (differential expansion) problems.

During the latter part of Phase I, the operational temperature requirement on the last 20 ft portion of the lead-in wire was relaxed from 2000^oF to −1200^oF. This revived the possibility of using *SS* lead-in wire, shorter pulse widths and correspondingly shorter coils than had previously been contemplated on the basis of the higher attenuation associated with a lead-in at 2000^oF. Experiments using 0. 5" coils and pulse widths of $\sim 5\,\mu$sec have shown the attenuation

8

to be less than 4 db/20 ft for SS 304 at $\sim 1250°$F (see Figs. 9 and 10). At room temperature the attenuation was found to be -8 db per 30 ft. Thus, a 50 ft SS 304 lead-in, 20 ft of which are at $-1200°$F, would attenuate the signal by about 8 t 4 or 12 db.

In another experiment, the attenuation in a 0.020" x 2" rhenium sensor was determined by observing the relative echo amplitudes at room temperature and at $\sim 5000°$F. The attenuation in this case was 8 db/inch at $5000°$F for a 0.5" coil and a pulse width of 5 psec.

Acoustic Isolation of the Lead-in Wire

In order to obtain acoustic isolation of the lead-in wire from the sheath, spacing wires were helically wound about 25 ft lengths of 0.063" SS 304 and 0.050" W lead-in wires. The resulting attenuation was found to be negligible if the ratio of spacing wire diameter to lead-in wire diameter was kept below $\sim 1/10$ (Fig. 11). Some increase in attenuation was observed when the spiral-clad wire was placed inside a SS 304 protective sheath. Subsequent heating to $1200°$F produced no significant increase in attenuation. In later tests, it was found that lead-in wires which are simply placed within the sheath in a loose fitting arrangement are sufficiently isolated acoustically.

Attenuating Effect of Liquid Sodium and 2" Radius Loops

It was early recognized that, if the lead-in wire were unsheathed, then over long immersion distances, the coupling to liquid sodium might attenuate the ultrasonic signals in the wire line. Two mechanisms are involved: viscous dampening, and lateral radiation which is a function of both the Poisson's ratio and the acoustic impedance mismatch from the line to sodium.

Now the viscosities of liquid sodium and water are comparable in the lower operating temperature range[4]-[7] (from its melting point to $750°$F, sodium exhibits the same range of viscosity values as water between $100°$F and $212°$F). Therefore, a simulation test was performed in which the last 20 ft of the 0.050" x 50' tungsten wire were immersed in a container filled with water at room temperature. The characteristic impedance of water at room temperature is equal to that of sodium at $\sim 1860°$F[7]. The viscosity of water at room temperature is more than 40% greater than that of liquid sodium at $208°$F. Both the viscous dampening and lateral radiation effects, however, were negligible, ($<$ 1db per 20 ft).

In a later test, the dampening effect due to lateral radiation from SS 304 wires into liquid sodium at temperatures as low as $\sim 700°F$ was also found to be negligible (see the section on field test). Torsional waves provide a useful alternative under those circumstances where the attenuating effects due to lateral radiation may be substantial. The present approach, however, is to place the sensor and lead-in wires in a protective sheath, and thus neither mechanism will be involved.

Additionally, two complete 2" radius loops were introduced above the immersion point, Fig. 12. The resulting oscilloscope displays are shown in Fig. 13. Clearly, the coiling produced a sizable reflection and reduced the amplitude of the end reflection (~ 3 db per loop). A truer simulation of access restrictions in the form of an S-shaped curve was later suggested by Argonne National Laboratory (ANL) personnel (see pp. **13,** 15 and Fig. 22). Subsequent measurements through the S-curve yielded a total signal attenuation of less than ~ 1.5 db.

Velocity Measurements in Cb, Cb-1% Zr, SS 304

Cb and Cb-1% Zr wires were tested to determine their velocity/temperature and amplitude/temperature characteristics, up to about $2000°F$. Both materials exhibited hysteresis effects, that is to say, the heating and cooling cycles yielded somewhat different values for the velocity at the same temperature. Moreover, the velocity of extensional waves was found to be relatively insensitive to temperature changes and appeared to increase in a certain range indicating an increase in Young's modulus in that range. Essentially the same results were obtained previously by Uva[8] on bulk specimens. The attenuation was also observed to be erratic. Accordingly, the use of Cb or Cb-1% Zr as sensors appears unwarranted.

The calibration curve for SS 304 is shown in Fig. 14. This curve was obtained by heating a length of SS 304 wire in an oven and monitoring the temperature with two chromel-alumel thermocouples brazed onto both ends of the sensor. The thermocouple beads provided the impedance mismatches to define the sensor. Figure 15 is a schematic of the oven calibration test. The two thermocouple temperatures remained within $2°F$ of each other throughout the test, indicating that the sensor length was nearly isothermal. Garofalo's data[9] are also included for comparison, but these data were obtained by static tests using bars in which Young's modulus may be expected to be different from drawn wire. That is to say, texturing may account for the small difference between our calibration on a wire and Garofalo's results in a bar.

Rhenium Velocity Measurements in UO_2 Environment

Rhenium sensors **0.030"** dia x **2"** long were placed in the ID of 2 tubes of depleted UO_2 each 0.144" OD x 0.035" ID **x 1"** long. The two tubes were positioned one on top of the other. The sub-assembly was housed in a 2" diameter Pyrex glass tube fitted with rubber stoppers at both ends. Most of the air in the glass tube ($\sim 98\%$) was then displaced by argon gas which was passed through the tube at a slow rate. The copper tubing passing through the stoppers was then crimped and cut, essentially sealing the glass tube. The rhenium sensor was then electrically self-heated[10].

At any given temperature, no changes in transit time with clock time were observed up to $\sim 2000°F$, indicating little or no effect of UO_2 on the sound velocity in rhenium. At higher temperatures, a mechanical and acoustic coupling developed between the sensor and the junction between the two UO_2 tubes. This coupling gave rise to a signal which interfered with both the weld and end echoes, terminating the experiment. To avoid this coupling problem in the actual fuel pin installation, as well as to minimize sensor/fuel interactions, we plan to use a sheath.

Cladding and Spiral Spacer Wires as Temperature Sensors

Tests were performed to determine the feasibility of using the SS 304 cladding and the 0.049" SS 304 spacer wire as temperature sensors. The objective is to use the cladding to measure its own temperature and the spiral spacer wire to measure sodium temperature next to the cladding. Initially, a 0.056" Remendur wire was spot welded onto the end of the spacer wire (Fig. 16). Transmission through the spacer wire with this arrangement was poor owing to the excessive length of the joint. Next, the spacer wire was removed, and a longer **0.047"** SS 304 wire was helically wound and spot welded to the tube in the same geometrical configuration but with a 6" length extending from the top of the tube (Fig. 16b). The resulting oscilloscope display is shown in Fig. 16c. It is seen that this construction results in identifiable signals from the spiral sensor.

In another test, a 0.056" Remendur wire was flattened at its end and brazed to the cladding, giving the transmission pattern shown in Fig. 17. Here also, the weld and end reflections are clearly identifiable. Thus, the feasibility of employing the cladding and spacer wire as temperature sensing elements has been established.

It should be noted, however, that these tests were conducted on an empty clad tubing of the type used in EBR-II fuel pin. The coupling effects of an internal sodium layer thermally bonding the UO_2 fuel to the tube in that type of capsule remain to be considered.

Field Tests at Argonne National Laboratory (ANL)

Sodium immersion tests were conducted in the oscillator rod facility at ANL during the week of April 29, 1968. These tests achieved the following objectives:

1. Demonstrated lead-in wire transmission through liquid sodium, with a −25 ft path of the lead-in wire either directly immersed in liquid sodium, or contained in an immersed sheath.

2. Determined the feasibility of using the immersed fuel cladding as a temperature sensor.

3. Determined the feasibility of using tungsten and/or SS 304 as lead-in wires. The tungsten wire was sheathed in a SS 304 tube.

4. Demonstrated the structural integrity of the ultrasonic thermometer with respect to the liquid sodium environment.

Figures 18 and 19 of the flange assembly show the relative positioning of the transducers, the magnetostrictive wires, and the lead-in wires. The bellows valves and needle valves were used to evacuate and backfill argon into all the tubes prior to startup. This precaution was observed to eliminate the possibility of an oxidation reaction in the event of a weld penetration or failure.

Four probes were simultaneously immersed in sodium as shown in Fig. 20. Probe #1 consisted of a sheathed 0. 063" SS 304 lead-in wire and a 0. 047" x 14" long SS 304 sensor. Probe #2 consisted of a sheathed 0. 050" dia tungsten lead-in wire etched to 0. 030" dia along the last 12" of its length to form a sensor. Probe #3 was not completed in time for the experiment; its position was plugged with a SS 304 rod (see Figs. 18 and 19). Probe #4 consisted of a 0. 063" SS 304 wire with a 12" long kinked sensor, and Probe #5 consisted of a 0. 063" SS 304 wire heliarc-welded to a 1/8" OD x 0. 020" wall SS 304 tube through a SS 304 conical transition element. A sheathed chromel-alumel thermocouple was used as a cross-check on the ultrasonic temperature measurement.

Assembly and check-out of all probes were completed by the morning of May 2nd, and the sodium fill was effected around 1620 hours, achieving a maximum temperature measured in the immersed sheathed thermocouple of $480^{o}F$ at 1730 hours. The system was then secured and the following morning at 0900 hours, a sodium temperature of $414^{o}F$ was recorded. Effort was then directed toward achieving the highest possible temperature during the remaining eight hours. At 1700 hours, the maximum achievable temperature as measured by the immersed thermocouple was $697^{o}F$.

Figure 21 is a plot of the normalized ultrasonic velocity versus the immersed thermocouple temperature for the bare and sheathed SS 304 sensors. Since thermal equilibrium was not maintained during the test*, and because the bare sensor apparently was close to the heated pipe wall, the temperature of the bare wire was slightly higher than that of the sheathed sensor. The laboratory calibration curve of Fig. 12 is included in the figure for comparison.

At the conclusion of the sodium immersion tests, a meeting was held with ANL personnel involved in the design of instrumentation assemblies for the EBR-II. During the discussion on geometrical configurations and accessibility of the EBR-11 core, the S-shaped curve in Fig. 22 was suggested as a feasible geometry for entry into the core. Subsequently, the S-shaped curve yielded a signal attenuation of ~1. 5 db as compared to the 3 db per full loop obtained earlier.

As a backup for the immersed chromel-alumel thermocouple and as a further cross-check, diametrically opposed longitudinal probes were attached near the bottom of the tank (see Appendix II). The longitudinal probes were used to obtain a through transmission measurement of the time taken for a 3 MHz pulse to traverse a diametral path in the vicinity of the probes. The longitudinal probes operated successfully and yielded temperatures in reasonable agreement with the values obtained from the immersed and wall-mounted thermocouples and the thin wire sensors.

Transducer Construction

The selection of construction materials for the transducer will obviously depend upon the operational environment. For operation at temperatures of $-150^{\circ}F$ or less in a very low radiation field intensity (i.e. , as achieved by using 50 ft lead-in wire), the transducer can be built with commercially available non-nuclear grade wire. Transducers of this type were built for the final system test described below and for the sodium immersion tests at ANL. The latter coils were constructed by silver brazing the threaded bases of Conax

---

*Temperatures measured with thermocouples mounted along the wall of the 10" pipe containing the sodium varied from one another and from the immersed thermocouple by as much as $100^{\circ}F$ during the test.

fittings onto one side of a subassembly and housed in a 0.538" OD SS 304 tube fitted at the opposite end with a BNC electrical connector (Fig. 23). Several types and sizes of commercially available wire were evaluated for transducer coil application. The most satisfactory compromise for a combined transmit/ receive coil from the standpoints of reliability, voltage breakdown, signal amplitude and stability was found in **#40** Niclad wire.

For transducer operation at higher temperatures in a radiation field, the problem is more difficult. The majority of the available high temperature electrically insulating materials for use in a nuclear environment are the ceramics. A very thin oxide layer on aluminum wire 0.009" dia was found to be a suitable insulator for a 0.5" long transducer coil. The Al_2O_3 layer was produced by two techniques, viz: oxidation in air and anodization in sulfuric acid solution. However, attempts to anodize sufficient lengths of 0.009" dia 99.999% pure aluminum wire for 3" long coils proved to be more difficult than had been anticipated on the basis of the previously successful results obtained with a 0.5" long coil, and precluded the expected testing of the aluminum transducer at ANL. The difficulty arose mainly because of the large number of turns necessary to accommodate the longer length of wire on *the* anode frame. This added contact area yielded bare spots which caused electric shorts between windings. Changes in geometry, voltage, and electrolyte concentration and temperature gave a more brittle oxide layer that flaked off upon winding.

The aluminum-coil transducer is limited to operation at temperatures less than $\sim 1000^o$F. For higher temperatures, 1000-2000°F, use of a zirconia base cement (Saureisen No. 29) was considered. However, attempts to wet wind transducer coils with this cement were unsuccessful. Other cement bases, viz., Al_2O_3, SiO_2, Na_2O could be considered for this purpose, **as** well as the possibility of using anodized tantalum. For the lower temperature range (< 1000°F) a 0.5" long anodized aluminum coil was found to give good signals. No degradation of the signals was observed when the coil was heated with a torch to about 800°F. However, for the ANL tests, it was decided that, to achieve low frequencies, 3" coils would be preferred, and **so** these experiments with Al transducer coils were abandoned for the time being.

It may also be possible to take advantage of high temperature, radiation resistant coils which Atomics International developed in connection with the SNAP program[11]. These coils, developed for another purpose, not magnetostriction, were wet-wound using various inorganic encapsulants and have been successfully tested to 1100°F in a radiation environment of 1.16×10^{19} nvt (E > 0.1 MeV) and 3.9×10^{10}R, gamma. However, the potential advantages

of anodized aluminum or tantalum coils over the insulation encapsulated type lie in a greater ease of fabrication, greater turns density (higher ampere-turns at less current) and, with the tantalum wire, higher maximum operating temperature **so** far **as** the coil is concerned.

Complete System Simulation Test

The complete ultrasonic temperature-measuring system was demonstrated on August 15, 1968.

The system configuration was as shown in Figs. 24, 25 and 26 and consisted of a pressure tight extensional wave transducer assembly, and a 0. 047'' dia **x** 20 ft SS 304 lead-in wire housed in a **0.125''** OD x 0. 020'' wall **x** 20 ft SS 304 protective sheath. The lead-in wire and its protective sheathing were bent in an S-shape containing two 2'' radius curves as shown to simulate accessibility conditions in reactor installations. A 0. **030''** dia **x 5''** Re wire was welded at the end of the SS 304 lead-in wire. The last 2'' of the Re wire acted as the temperature sensor. A notch, 3'' from the SS 304/Re weld, provided the first echo. The sensor was placed in a 0. 065'' dia **x** 0. 006'' wall x 6'' long Ta tube. This tube was heated electrically to give a maximum sensor temperature of 5000°F.

An automatic instrument (Fig. 2) was used to read the transit time in the sensor to 0.1 psec. The temperature was determined from a previously calibrated graph of the sound velocity in Re versus temperature. At 5000°F, the end echo was attenuated only about 16 db compared to its value at room temperature. Thus there was ample signal strength even at the highest temperature of interest. The list on the next page summarizes the sources of attenuation in the complete line, **for** pulse widths of 5 psec and 1/2'' coils.

Additionally, the attenuation in **SS** 304 at room temperature was determined by launching extensional waves simultaneously in a one foot wire and a 30 foot wire as shown in Fig. 27. The ratio of echo amplitudes indicated an attenuation of -8 db per 30 feet. Further, the signal amplitude of a prototype 1/2'' coil was observed to be $\sim$4V in very short lines at room temperature. Additionally, the effects of low frequency vibration were shown to be negligible in experiments wherein a doorbell buzzer was used to vibrate an ultrasonic sheath and line (Fig. 28). This test was witnessed by AEC personnel with extensional waves on the line; it was later repeated with torsional waves on a different line, with essentially similar results , namely the low frequency noise, although of large amplitude, did not degrade the high frequency ultrasonic signal.

Finally, the transducer was successfully tested for pressure tightness at 100 psig.

Summarizing the losses in the ultrasonic system*, we find:

a) Room temperature, 50 ft of SS 304 at 8 db per 30 ft.. 14   db

b) At 1200°F, 20 ft of SS 304 (additional attenuation due to heating up to the maximum sodium temperature expected). **4**

c) At 5000°F, 2" of rhenium.................................. 16

d) S-shape containing bends with 2" radius of curvature.. .... 1. 5

Total losses   35.5 db

If the above loss figure is rounded off to 40 db (i.e., amplitude ratio of 100) the transducer output for a detection threshold of -10 mV must be on the order of 1 volt at room temperature for a short, relatively attenuation - free line. Since signals of at least this magnitude have been obtained (e. g. , 4V - see above), the problem of attenuation no longer appears significant.

*For pulse widths of 5 psec and 1/2" coils

CONCLUSIONS

A complete ultrasonic system was designed and constructed to automatically determine the fuel, cladding and coolant temperatures for the development and operation of advanced liquid metal cooled fast breeder reactors (LMFBR). The complete system was successfully tested in the laboratory under conditions simulating the high temperature environmental conditions, and the geometrical restrictions on accessibility obtained in LMFBR's. Specifically, these conditions for fuel temperature determinations are:

a) A maximum sensor operating temperature of -5000°F.

b) A sheathed 50 ft lead-in wire, 20 ft of which are at $\sim 1200^{o}$F.

c) An S-shaped curve containing two 2" radius curves to simulate accessibility conditions,

d) **A** pressure and leak-tight feedthrough capable of withstanding pressures of 100 psig.

e) An automatic electronic read-out instrument capable of measuring transit time to $\pm$ 0.1 μ sec.

Additionally, the following items have been demonstrated:

1) The structural integrity of the ultrasonic thermometer with respect to a liquid sodium environment.

2) The feasibility of using the cladding itself as an ultrasonic temperature sensor to measure its own temperature. The effect on cladding echoes of the fuel and sodium inside the cladding, however, remains to be investigated.

3) The feasibility of using the spiral spacer wire to determine the coolant temperature.

4) The feasibility of using anodized aluminum transducers up to -1000°F. More work needs to be done to determine the characteristics of such transducers in a combined high temperature, nuclear radiation environment.

5) The effect of UO_2 on the speed of sound in rhenium is negligible up to at least $\sim 2000^{o}$F, at least for brief exposures.

6) If a wire is loosely placed in a sheath, the ultrasonic coupling between wire and sheath is negligibly small.

7) The loss of ultrasonic energy in a bare 20 foot SS 304 wire immersed in liquid sodium is negligibly small for pulse widths of $\sim$ 37 μ sec.

8) Low frequency mechanical vibration does not noticeably affect the temperature measurements.

The experimental results demonstrate that the goals of Phase I have been met.

RECOMMENDATIONS FOR FUTURE WORK

It is recommended that, in Phase 11, the ultrasonic system constructed and laboratory tested in Phase I be installed in a selected liquid metal nuclear reactor facility to ultrasonically measure in-core temperature. The main emphasis should be placed on fuel meat temperature, particularly at the fuel pin centerline.   In-core tests at Oak Ridge National Laboratory can subject the ultrasonic system to the combined environment of mixed oxide fuels, sodium, intense nuclear radiation, 10^{13} n/cm^2-sec (fast) and 10^{14} n/cm^2-sec (thermal) integrating in a typical seven-week test to fluences of nearly 10^{19} nvt (fast) and 10^{20} (thermal) and temperatures up to the maximum levels available at this facility, i.e,, up to $\sim 4500^{\circ}$F.   Radiation effects on the ultrasonic system should be determined by combinations of before-and-after tests, tests on control vs irradiated .wires, comparisons with independent measures of temperature, and by tests on Re/Os wires simulating the composition of a Re sensor partly transmuted to Os after long-term exposure to radiation.

ACKNOWLEDGMENTS

APPENDIX I

Sensitivity of the Ultrasonic Temperature Measurement

To compute the minimum sensor length **L** that provides a desired sensitivity, we may proceed as follows.

Since the round trip transit time, t, in the sensor is given by

$$t = \frac{2L}{V} \tag{1}$$

where V is the sound velocity, we have

$$\frac{dt}{dT} = -\frac{2L}{V^2}\frac{dV}{dT}$$

or

$$L = -\frac{1}{2}\frac{V^2\,dt}{dV} \approx -\frac{1}{2}\frac{V^2\,\Delta t}{\Delta V} \tag{2}$$

where Δt is the uncertainty in time measurement and ΔV is the change in the speed of sound in an interval ΔT about a temperature T.

As a numerical illustration, suppose the desired sensitivity is $\pm 1\%$ at **2760°C = 5000°F**. From Fig. 3, we have for an extensional wave,

$$V_o(5000°F) = 3.23 \times 10^5 \text{ cm/sec}; \quad \frac{dV}{dT}(5000°F) \approx -40 \text{ cm/sec°F}$$

$$\therefore \Delta V_o = -40 \times 50 = -2{,}000 \text{ cm/sec.}$$

If $\Delta t = \pm 0.1$ psec, then

$$L = \left(\frac{1}{2}\right)\frac{(3.23 \times 10^5)^2\,(0.1 \times 10^{-6})}{2 \times 10^3}$$

$$= 2.61 \text{ cm or approximately 1 inch.}$$

For a 2.61 cm sensor, the round trip transit time at room temperature where

$$V_o = 4.92 \text{ x } 10^5 \text{ cm/sec},$$

is

$$t = \frac{2 \text{ x } 2.61}{4.92 \text{ x } 10^5} \approx 10.6 \text{ psec}$$

The maximum allowable pulse width is limited by possible interference of the echo side lobes (see Fig. 5) which could result in pulse distortion and hence cause time measurement errors. In practice, it turns out that the maximum allowable pulse width is approximately one third the round trip transit time, in this case 3.5 psec, which corresponds to a frequency bandwidth of -283 kHz.

Possible Means of Increasing Sensitivity

At temperatures lower than 5000^oF, L = 1 inch yields less sensitivity than 1%. Note that at the lower temperature where sensitivity is low, the attenuation is also low, and so one can compensate for the low sensitivity by using multiple echoes in a short sensor. Until limited by attenuation, then, one may resort acoustically to longer sensors, torsional waver ,see **Fig.** 29) and/or multiple echoes. **As** an example, in a recent industrial application where the temperature of molten nickel-base alloy was to be measured, the fourth multiple extensional wave echo in a 2" Re sensor provided a sensitivity of about 10^oF at $2800 \cdot 3000^o\text{F}$.

It can be shown that the absolute value of the maximum ratio of the n th echo amplitude to the amplitude of the incident wave is given by

$$\left| \frac{A_n}{A_o} \right| = \left| \frac{r - 1}{r + 1} \right|^{n-2} \frac{4r}{(r + 1)^2} \tag{3}$$

where

$$r = (n\text{-}1) \pm \sqrt{n(n\text{-}2)} \tag{4}$$

r = impedance ratio = Z_b/Z_a (see Fig. 5a caption)
n = echo number

20

Values of $\left|A_n/A_o\right|$ and r are given in Table 1 and plotted in
Fig. 5a as functions of n. As an example of the use of these quantities,
consider the case where an increase in temperature sensitivity is to be
obtained by measuring the transit time between the first and third echoes.
From Table 1 and Fig. 5a the maximum amplitude of the third echo is
0.385V for an incident wave amplitude corresponding to 1V. Two im-
pedance ratios will yield this value (via. 3.73 and 0.268, respectively)
indicating that there are two geometric configurations that can achieve
this purpose (d_b/d_a = 1.93 or 0.518) the only difference being a phase
reversal.

Table 1

n	r1	r2	$\left(d_b/d_a\right)_1$	$\left(d_b/d_a\right)_2$	$\left(A_n/A_o\right)_1$	$\left(A_n/A_o\right)_2$
2	1	1	1	1	-1	-1
3	3.73	0.268	1.93	0.518	-0.385	+0.385
4	5.83	0.172	2.41	0.414	-0.250	-0.250
5	7.87	0.127	2.81	0.356	-0.186	to.186
6	9.90	0.101	3.15	0.318	-0.148	-0.148
7	11.92	0.0839	3.45	0.290	-0.123	+0.123
8	13.93	0.0718	3.73	0.268	-0.105	-0.105
9	15.94	0.0627	3.99	0.250	-0.092	+0.092
10	17.94	0.0557	4.24	0.236	-0.082	-0.082

Ultrasonic Temperature Compared to Average Temperature

The fact that a measurement of sound velocity averages the tem-
perature over the sensor length often is disconcerting to workers more
familiar with point-type measurement of temperature obtained with
thermocouples or optical pyrometers. The authors have shown, however,
that the ultrasonic temperature and the arithmetic mean temperature over
the sensor path usually agree within 1% or better[1, 12, 14, 15, 16]. The
question of obtaining temperature profiles from differential path measure-
ments has also been treated analytically and experimentally[16]. A more
detailed treatment of temperature sensitivity and averaging will be pub-
lished elsewhere[12].

APPENDIX 11

Ultrasonic Measurements in Liquid Sodium

At ANL, **two** longitudinal wave probes were coupled to the exterior of the 10" diameter pipe as shown in Figs. 30 and 31. A 3 MHz pulse was transmitted through the diametral path. The transit time for through transmission **was** then related to the mean temperature across the diameter through the sodium V(T) characteristic shown in Fig. 32. The calculations are similar to those shown in Appendix I.

$$t = \frac{L}{V}$$

$$\frac{dt}{dT} = -\frac{L}{V^2} \frac{dV}{dT}$$

For L = 10", at 600°F, the uncertainty in temperature for a time resolution of ± 0.01 μsec is dT $\approx \pm 0.8^{\circ}$F, or better than 1°F.

Significantly, no difficulty was experienced in coupling to the OD of the hot **SS** pipe, nor from the ID of the pipe to the liquid sodium. Apparently, the sodium wetted the pipe. After *the* tests were over, the ultrasonic probes were easily dismounted from their temporary positions, by loosening a clamp.

Figure 33 illustrates the shift in transit time. The significance of these results is that they establish the feasibility of ultrasonically measuring the sodium temperature **by** a method that does not interfere with normal sodium **flow** and requires no hole in the pipe. Thus, it may be possible to measure the inlet and/or outlet coolant temperatures for extended periods (e. g., up to **5** years or more). Instrumentation embodying this concept could, if required, be attached to existing sodium lines for evaluation under operation conditions.

This appendix includes a general discussion of circuitry in block diagram form, and a list of front and rear panel controls and connectors.

_____ ı tic Measu _____ of Pulse · t 'i _____

Referring now to Fig. 34, a low frequency pulse generator 51 times the generation of interrogating acoustic pulses. Pulses provided by generator 51 are applied, through an element 53 which provides a short delay, to a transducer 55. The transducer 55 is also electrically coupled to a receiver 61 which detects echo pulses reflected from the sensors 57 and 59. The undelayed pulse signal provided by generator 51 is also applied to receiver 61 as an inhibit signal to prevent the receiver from responding to or being overloaded by the interrogating pulse.

Echo pulses detected by the receiver 61 are provided to a pair of leads 63 and 65. A pair of switches SW1 and SW2 permit the signals applied to leads 63 and 65 to be taken either directly from the receiver or through an inverter 67 so that the pulses supplied to the leads will be of proper polarity (AB, $\overline{AB}$, $\overline{A}B$, AB) to correctly operate the following circuitry. Similarly, a pair of switches SW3 and SW4 permit the amplitudes of the signals to be either adjusted or not adjusted by means of respective **ECHO BOOST** amplifiers as indicated at 69 and 71. The echo pulses reflected back from ultrasonic sensors may be of different amplitudes and polarities depending upon the acoustic impedances of the materials employed. The switches SW1-SW4 permit any of various possible combinations of desired pulses to be utilized by this apparatus.

The interrogating pulse signal which is applied to the transducer 55 is also applied to 73 which provides a preselectable delay, which delay can be varied over a substantial range. The output signal provided by the delay element 73 is applied to one of the inputs of a flip-flop circuit 75 which in turn controls a gate 77. Gate 77 selectively applies the echo pulse signal available at line 65 to a gated sample and hold circuit 79 and a discriminator circuit 81. The sample and hold circuit 79, when gated on, utilizes the pulse signals applied thereto and samples the amplitudes of echo pulses applied thereto through gate 77 and provides a voltage substantially equal to the peak amplitude of the echo pulses. This peak voltage is applied to discriminator 81.

Discriminator 81 compares the echo pulse signal passed by gate 77 with the peak voltage provided by the sample and hold circuit 79 and provides a sharply switched output voltage when the echo pulse signal exceeds a preselected portion, e. g., 70%, (or any other percentage in the range 50-90%) of the peak voltage.

Accordingly, the output signal from discriminator 81 is a square wave signal in which each square wave pulse has a duration substantially equal to the duration of that portion of the corresponding echo pulse which is above 70% of the peak amplitude (see Fig. 5b, lower trace). In other words, the peak sample and hold circuit 79 and the discriminator 81 together operate as a squaring circuit for selected echo pulse signals passed by gate 77. The output signal from the discriminator 81 is applied to the other input of flip-flop circuit 75 **so** that the gate 79 is closed at the trailing edge of each square wave output pulse.

The output signal from discriminator 81 is also applied to a circuit element 83 which provides a preselectable delay in the manner described previously with reference to the variable delay element 73. The output signal from delay element 83 is applied to one of the inputs of a flip-flop circuit 85 which controls a gate 87, the signal being applied **so** that the gate 87 is opened at the end of the delay provided by the circuit element 83.

Gate 87 controls the application of the echo pulse signal available at lead 63 to a peak sample and hold circuit 89 and a discriminator 91 which are substantially identical with the circuit elements 79 and 8-1 described previously and which utilize echo pulse signals applied thereto in similar manner. In other words, these elements operate tb **"square"** selected echo pulses passed by the gate 87. The square wave output signal provided by discriminator 91 is applied to the other input of flip-flop 85 **so** as to close the gate 87 at the trailing edge of each square wave output pulse.

The peak amplitude signal provided by the peak sample and hold circuits 79 and 89 are also provided at respective output terminals 80 and 90 **so** that amplitude and attenuation measurements of the selected pulses may be made. The square wave output signal provided by discriminator 81 directly controls a gate 93 and is also applied to one of the input terminals of a flip-flop 95. The square wave output signal provided by the discriminator 91 directly controls a gate 97 and is also applied, through an inverter 99, to the other input terminal of flip-flop 95. The output signal from flip-flop 95 controls a gate 101.

A clock oscillator 103 provides, at a lead 105, an a. c. signal at a predetermined, fixed frequency, e. g., 10 megahertz. The signal provided at lead 105 is applied to a binary counter 107 which provides, at a lead 109, an a. c. signal at a frequency which is half that provided at the lead 105, e. g., 5 megahertz. **As** is described in greater detail below, the a. c. signals provided at leads 105 and **109** function as clock signals which establish a time base for timing the intervals between echo pulses. Gates 93 and 97 control the application of the lower frequency

24

a. c. signal from lead 109 to respective inputs of an OR gate 111 while the gate 101 controls the application of the higher frequency signal from lead 105 to a third input of OR gate 111. The output signal from the OR gate 111, which comprises the sum of the various gated clock signals applied thereto, is selectively passed by a gate 115 to a divide-by-10 counter 117 which in turn drives a display counter 119. The oscillator 103, the counters 117 and 119 and the various gated controlling the clock signals thus comprise a digital clock.

The square wave output signal provided by discriminator 91 is also applied to a counter 125 which has 12 distinct states. Counter 125 in turn times the operation of a program control circuit 127 which, as will be explained in greater detail below, controls the sequence of operations of the apparatus of Fig. **40** following successive sensor interrogation pulses. In particular, the program control circuit 127 controls: the gating of the peak sample and hold circuits 79 and 89; the operation of the gate 115 which controls the application of the clock signals to the counters 117 and 119; and the resetting of the counter 119.

The operation of this apparatus is substantially as follows. The preselectable delay provided by element 73 is adjusted **so** that the **BLANKING** DELAY is slightly shorter than the nominal interval between the interrogating pulse and the first of the preselected pair of echo pulses. Similarly, the preselectable delay provided by element 83 is adjusted **so** that the ECHO SELECT is slightly shorter than the nominal interval between the **two** echo pulses which constitute the preselected pair. Accordingly, following the generation of an interrogating pulse, the gate 77 is opened just in time to admit the first of the preselected echo pulses to the peak sample and hold circuit 79. The trailing edge of the resultant square wave signal provided by discriminator 81 then resets the flip-flop 75 closing gate 77 **so** that this portion of the circuitry is no longer responsive to received echo pulses.

The trailing edge of the square wave pulse provided by discriminator 81 also triggers the variable delay circuit 83. Delay circuit 83 in turn, by triggering the flip-flop 85, opens the gate 87 just in time to admit the second of the preselected pair of pulses to the peak sample and hold circuit 89. The trailing edge of the resultant square wave pulse provided by discriminator 91 then resets the flip-flop 85 thereby closing the gate 87 **so** that this portion of the circuitry also is then no longer sensitive to received echo pulses. From the foregoing, it can be seen that the peak sample and hold circuits 79 and 89 and the discriminators 81 and 91 are activated only by respective ones of the preselected pulses.

The square wave signals provided by discriminator 91 also advance

the cycle counter 125 which drives the program control network 127. The operation of the program control network 127 is such that the peak sample and hold circuits 79 and 89 are gated into operation or activated only during the first two cycles in the overall sequence of 12 interrogation cycles. Thus, during the first **two** cycles, the circuits 79 and 89 sample the respective echo pulses and provide a signal representative of the peak amplitudes of those pulses. Accordingly, during the next 10 interrogation cycles, the discriminators 81 and 91 provide square wave output signals having durations equal to the portion of time which the respective echo pulses exceed a predetermined portion of the previously established peak amplitude. **As** will be apparent hereinafter, these square wave signals are taken as defining the durations of the respective echo pulses (again see Fig. 5b, lower trace).

The square wave signal provided by discriminator 81 opens the gate 93 for the duration of the respective preselected echo pulse, thereby causing the half frequency signal from lead 109 to be applied to the OR gate 111 during this interval. At the end of this interval, i. e., at the trailing edge of the square wave pulse provided by discriminator 81, the flip-flop 95 is triggered, opening the gate 101. The opening of gate 101 allows the full frequency a. c. signal provided by oscillator 103 to be applied to the OR gate 111.

The square wave output signal from discriminator 91, being applied to the other input of flip-flop 95 through inverter 99, causes the flip-flop to close gate 101 at the leading edge of the square wave signal provided by discriminator 91, i. e. , at the beginning of the second of the preselected echo pulses. Simultaneously, this leading edge of the square wave pulse provided by discriminator 91 opens the gate 97 **so** that the half frequency signal provided at lead 109 is then applied to the OR gate 111. It can thus be seen that the output signal from the OR gate 111 comprises the half frequency clock signal for the duration of the first preselected echo pulse; the full frequency clock signal from the end of the first of the preselected pulses to the beginning of the second preselected pulse; and the half frequency clock signal again for the duration of the second preselected echo pulse.

The program control network 127 controls the gate 115 **so** that the output signal from the OR gate 111 is applied to the counters 117 and 119 for the last ten interrogation cycles in each full sequence of the cycle counter 125. Since the display counter 119 is preceded by the divide-by-ten counter 117, it will be understood that the count displayed will thus represent the average of the counts taken over the ten interrogation cycles. Further, since the counting is based on the half frequency signal for the whole duration of each of the echo pulses,

26

the count displayed will be substantially equal to that which would occur if the measurement were taken between the centerlines of the square wave signals defining the echo widths. In practice, this time closely corresponds to the time from the exact peak of the first of the preselected echo pulses to the exact peak of the second preselected echo pulse. In a broad sense then, the output signal from the discriminator 81 starts the digital clock and the output signal from discriminator 91 stops the clock.

From the foregoing, it can be seen that the count displayed by counter 119 is an accurate measurement of the time interval between a preselected pair of pulses and that the particular pulses which are pre-selected can be easily changed by appropriately preselecting the delays provided by the variable delay elements 73 and 83, i. e., front panel **BLANKING** DELAY and ECHO SELECT switches. Thus the apparatus of Fig. **34** can be used with a variety of sensors to measure a desired sensor delay interval, without being affected by the various other pulses which are present in the transducer signal, and different sensor elements within a given one of the probes can be selected by appropriately selecting the nominal delays which select the pair of pulses between which the time interval is measured.

If desired, nine preset delays, each of which corresponds to a respective sensor, may be preselected and adjusted by means of nine potentiometers which control the RC time constants.

The apparatus of Fig. **34** may also select between different sensed parameters in a probe in which ultrasonic pulses are transmitted in dif-ferent modes and the different modes experience correspondingly different delays. For example, a Joule-Weidemann transducer generates both torsional waves and extensional waves. The velocity of the torsional waves depends upon the shear modulus of the sensor material and the velocity of the extensional waves depends upon the Young's modulus of the sensor material. Accordingly, ambient conditions which affect these parameters differently may be sensed with a single sensor element.

Similarly, this apparatus may be utilized to select particular information-bearing pulses in a system in which transducers are employed at both ends of a probe assembly and the desired information is provided by a combination of reflected and through-transmitted signal pulses.

The apparatus of Fig. **34** also facilitates the selection of particular pulses in a series of pulses in systems in which the desired information is represented by the amplitudes of the selected pulses, this information being provided at the terminals 80 and 90 which provide signals representing

the peak amplitudes of the respective pulses and thus permit attenuation measurements.

Another application of the apparatus of Fig. **34** is in effectively increasing the magnitude of the measured delay and thereby increasing the sensitivity of measurement of the sensed parameter. **As** mentioned previously, an ultrasonic pulse may undergo multiple interval reflections within a single sensor element. By choosing an appropriate pair of pulses in the sequence of pulses generated, the measurement obtained can reflect the delay or attenuation resulting from a plurality of passes through the sensor element and thus the effect of the sensed parameter or ambient condition is amplified **so** that a more accurate measurement is obtained.

Front Panel Controls and Connectors (see Figs. 2, **34**)

Name	Function
PULSE WIDTH	Vernier adjusts transmit pulse width from 3 to 30 psec range.
POWER	Detent turns power on;. vernier increases transmit pulse magnitude from 0 to about -30 V in clockwise direction, to provide a current pulse up to at least 1.2 A max.
T - T/R	Toggle switch selects transmit only (T) mode or transmit/receive (T/R) mode.
BLANKING DELAY	Ten-position detent switch selects 1 of 9 internally RC adjustable and pre-set delay flop suppression gate widths, or, in EXT position, selects externally controlled suppression gate width. Internal R adjustment accessible through top cover slots; pedestal corresponding to selected blanking delay gate width may be monitored from rear panel SELECTOR MONITOR BNC.
RECEIVER GAIN	Four-position detent selects echo amplitude range ($<$10 mV, 10-100 mV, 100-1000 mV, 1-10 V), and concentric vernier adjusts gain within selected range. Signals thereby amplified may be monitored at rear panel RECEIVER MONITOR BNC.
POLARITY	Four-position detent selects polarity of echo pair between which time is to be measured (AB, $\overline{AB}$, $\overline{A}$B, AB).
ECHO SELECT	Detent and vernier concentric with POLARITY switch, to control a second delay flop suppression gate width from 10 to 100 psec when turned clockwise, or to reduce second gate width to zero, when turned fully CCW to off position.
PPS	Three-position toggle switch, to control pulse repetition frequency, to 60, 120 or, in EXT position, to permit external control from 30 to 200 pps.
ECHO BOOST	Pair of toggle switches for first and second selected echoes A and B, respectively, to boost or amplify either or both of said echoes by a factor of 3.
FRONTPANEL CONNECTORS	Two BNC's, labeled TRANSMIT AND RECEIVE.
FRONT PANEL DISPLAY	Displays transit time, measured between centerlines of selected echoes, to 0.1 psec.

Rear Panel Controls and Connectors

Name	Function
CONTINUOUS MOMENTARY EXT TRIG	Two-position toggle switch, to select pulsing mode. When CONTINUOUS is selected, prf is controlled by front panel 60 or 120 pps, or EXT 30 to 200 pps. When MOMENTARY is selected, push-button triggers a single measurement sequence of twelve pulses, or, alternatively, logic level pulse applied to rear panel EXT TRIG BNC triggers a single measurement sequence of twelve pulses.
CLOCK	Buffered **5 V** output, derived from 10 MHz crystal.
RECEIVER MONITOR	Output of receiver amplifier, showing signal prior to ECHO BOOST amplifiers.
SYNC	**4** V ± 1V pulse into a minimum load of 1K occurring at beginning of transmitter pulse (main bang).
EXT PRF	DTL gate, logic levels, controls prf from 30 to 200 pps, provided front panel **PPS** toggle is switched left to EXT position.
ANALOG OUT	Output (J24) of digital-to-analog converter, 0-10 V, up to 20 mA, accuracy 0.05% proportional to transit time, for recording on strip chart or multipoint recorder.
SELECTOR MONITOR	Group of pedestals showing gate widths of BLANKING DELAY and ECHO SELECT delay flop suppressors, as well as indicating time interval that each selected echo exceeds comparison level in the range 50-90% of peak sampled-and-held level (see Fig. 5b).
COUNTER DATA	16 line BCD counter output with logic levels of Logic "1", ± 4. 5 V ± 0.5 V in series with 3600 ohms; Logic "0", ± 0. 5 V at 10 mA. Also, at pin **24,** "end of measurement" signal, ± 5V ± 0. 5 V, corresponding to end of group of 12 main bangs and their resultant echoes. Also, at pin 22, fault signal (logic level "1" means fault; logic level "0" means no fault) to indicate malfunction. Pin 23 is ground.

Binary weighting for 16 line BCD digital data output is as follows:

Line	Weight	Line	Weight	Line	Weight	Line	Weight
1	1	5	10	9	100	13	1000
2	2	6	20	10	200	14	2000
3	4	7	40	11	400	15	4000
4	8	8	80	12	800	16	8000

Name	Function
EXTERNAL TIMING	For external control of PULSE WIDTH and BLANKING DELAY time intervals. PULSE WIDTH is controlled by turning front panel PULSE WIDTH knob to maximum (1K) position, and connecting 100K potentiometer between pins 5 and 6, thereby shunting 1K potentiometer setting. BLANKING DELAY is controlled externally by switching front panel BLANKING DELAY knob to EXT position, and, on EXTERNAL TIMING connector, connect ends of 5K potentiometer between pins 2 and 3, and arm of potentiometer to pin 1. Also, pin 22 is ground; 23 is B echo level monitor and 24 is A echo level monitor including A and/or B amplifications which may have been switched IN at ECHO BOOST controls.

REFERENCES

1. Lynnworth, L. C. and Carnevale, E. H., "Ultrasonic Temperature Measuring Device," NASA CR-72339 (Aug. 1967). See also M. S. McDonough et al., "Ultrasonic Measurement of Core Material Temperature," NASA CR-72395 (Dec. 1967); NASA CR-72395, Job 66, Phase II Report (Aug. 1968).

2. See, for example, Tzannes, 'N. S., Wiedemann Sonic Delay Line, Ph. D. Thesis, John Hopkins Univ. , (1966); "Joule and Wiedemann Effects - The Simultaneous Generation of Longitudinal and Torsional Stress Pulses in Magnetostrictive Materials," IEEE Trans. on Sonics and Ultrasonics, SU-13 (2) 33-41 (July 1966). See also Brockelsby, C. F., et al, Ultrasonic Delay Lines, Iliffe Books, Ltd., London (1963), Chapter 6 and Davidson, S., "Wire and Strip Delay Lines, "Ultrasonics 3 (3) 136-146 (July-Sept. 1965).

3. Mason, W. P., Physical Acoustics and the Properties of Solids, Bell Laboratories Series, Van Nostrand, (1958), Princeton, N. J. See also NASA CR-72339, Ref. 1; J. R. Hutchinson and C., M. Percival, "Higher Modes of Longitudinal Wave Propagation in Thin Rods," J. Acoust. Soc. Amer. 44 (5) 1204-1210 (Nov. 1968).

4. Liquid-Metals Handbook, Sodium-NaK Supplement AED (July 1955), p. 26.

5. Grosse, A. V. , "Viscosities of Liquid Sodium and Potassium from Their Melting Points to Their Critical Points," Science, 147, 1438-1440.

6. Perry, J. H. , Chemical Engineers' Handbook, McGraw-Hill, Fourth Edition, (1963).

7. Golden, G. H., Tokar, J. V., Thermophysical Properties of Sodium, Argonne National Laboratory Report ANL-7323 (Aug. 1967).

8. Uva, S., An Ultrasonic Determination of Elastic Moduli, MS Thesis 1964, Boston College, Boston, Mass. See also Carnevale, E. H. and Lynnworth, L. C., "Ultrasonic Measurements from 1000 to 10,000°K," 5e Congress International d' Acoustique, Liège (1965); Carnevale, E. H., Aerospace Measurement Techniques, NASA SP-132, 73-103 (1967).

9. Garofalo, F., "Temperature Dependence of the Elastic Moduli of Several Stainless Steels," ASTM Preprint #81. Paper presented at the Sixty-Third Annual Meeting of the Society (June 25 - July 1, 1960).

10. Lynnworth, L. C., pat, pending; "Use of Ultrasonics for High Temperature Measurements," to be published in Materials Eval. 27 (1969).

11. Long, W. G. and Keating, W. E,, "Development of Electrical Insulation Systems for 1100°F and 10,000 Hour Service," Reprint from Insulation, (1966), Lake Publishing Corp. This work was performed under AEC Contract AT(11-1)-GEN-8.

12. Fam, S. S. , "Some Aspects of Thin Wire Ultrasonic Thermometry and its Applications," - to be published.

13. Lynnworth, L.' C., Carnevale, E. H. , McDonough, M. S., and Fam, S. S., "Ultrasonic Thermometry for Nuclear Reactors," IEEE 15th Nuclear Science Symposium, Montreal, Canada, Oct. 23-25, 1968. IEEE Trans. Nucl. Science (Feb. 1969).

14. Lynnworth, L. C,, Carnevale, E. H, and Carey, C. A., "Ultrasonic Thermometry in Solids and Gases at Elevated Temperatures," paper III-B, in Proc. Fifth Temperature Measurements Society Conf. and Exhibit, Hawthorne, Calif. (March 14-15, 1967).

15. Lynnworth, L, C, and Carnevale, E. H,, "Ultrasonic Testing of Solids at Elevated Temperatures," Proc. Fifth International Conference on Nondestructive Testing, Montreal, Canada (May 21-26, 1967), 300-307.

16. Carnevale, E. H., Larson, G., Lynnworth, L. C, , Carey, C., Panaro, M. and Marshall, T., "Experimental Determination of Transport Properties of High Temperature Gases," NASA CR-789, Phys. Fluids 3040-3048, (June 1967).

17. Lynnworth, L. C., "Ultrasonic Probes Using Shear Wave Crystals, Principles," Materials Eval. 25(12) 265-277 (Dec. 1967); "Part 11 - Applications," in Proceedings of the Sixth Symposium on Non-destructive Evaluation of Aerospace and .Weapons Systems components and Materials, San Antonio, Texas (April 17-19, 1967), 323-3 1.
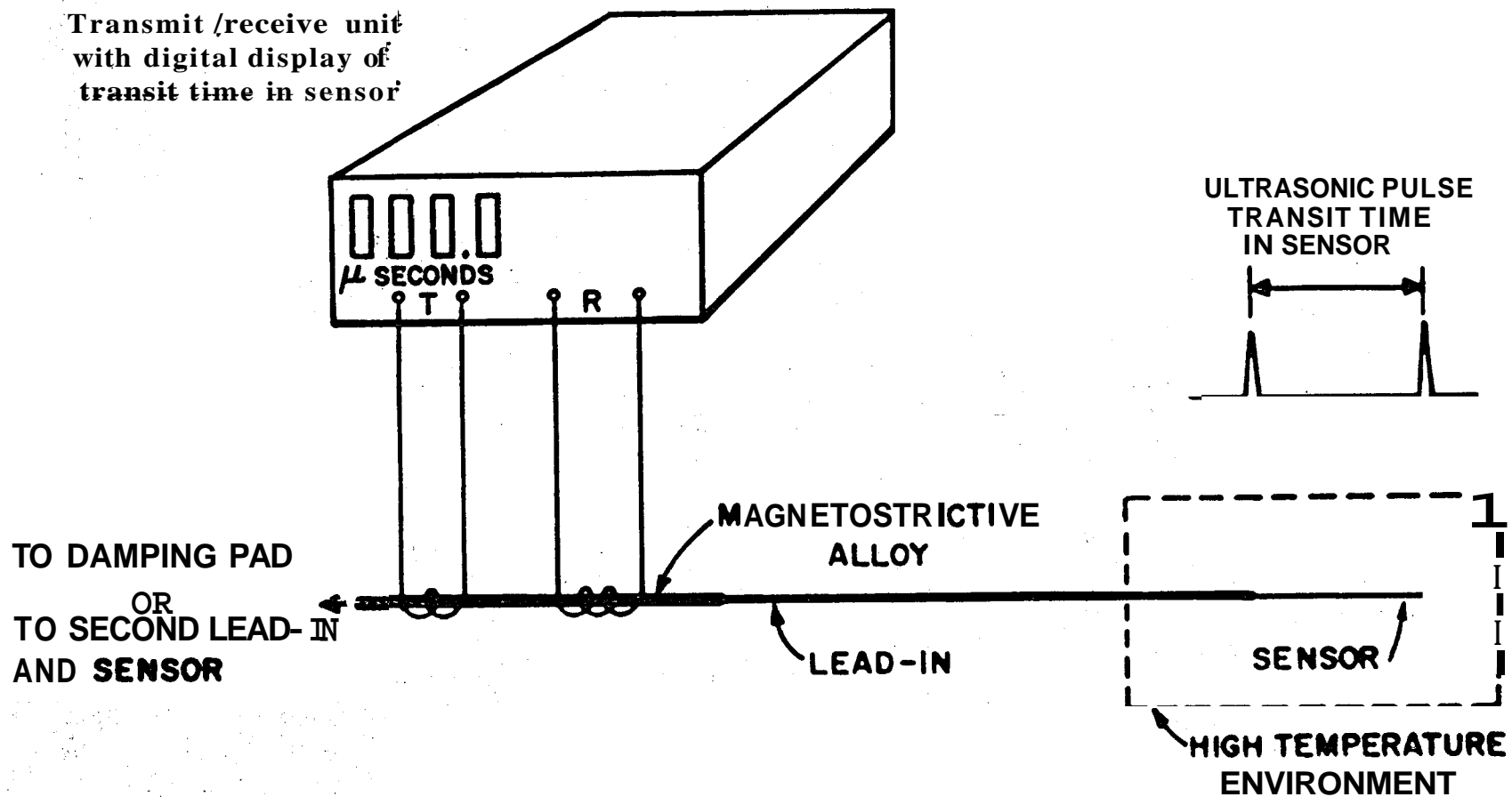
Figure 1. Schematic of automatic measurement of pulse transit time in sensor.

Fig. 2. Instrument automatically measures transit $\smile$ in sensor to 0.1 μsec.

Figure 3. Velocity vs temperature in Mo, Re, W, Ta and SS 304.
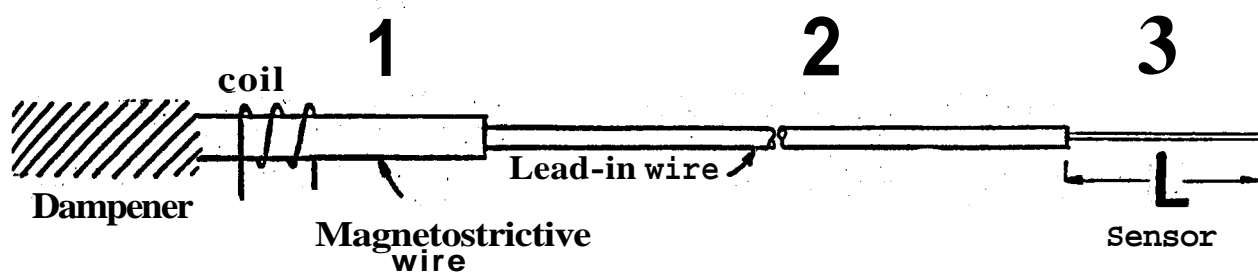
Figure 4. Schematic of basic ultrasonic thermometer.

Fig. 5(a). Impedance ratio and maximum echo amplitude vs. echo number.

side lobes   reverberations in sensor

RECEIVER MONITOR

SELECTOR MONITOR

base line

|← — — — — BLANKING DELAY ————→|
pedestal

ECHO
SELECT
pedestal

Echo A
EVALUATOR
pedestal

Echo B
EVALUATOR
pedestal
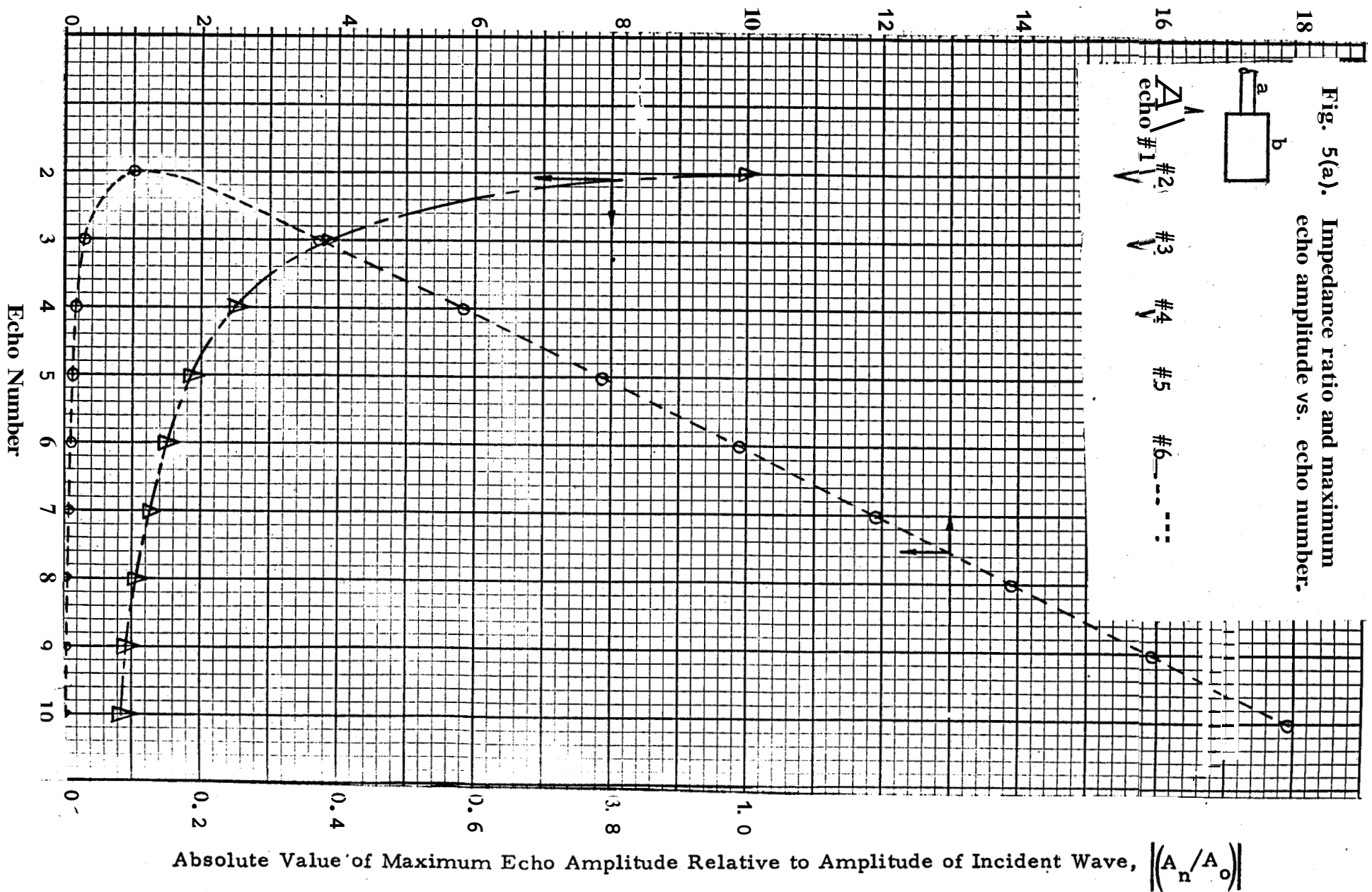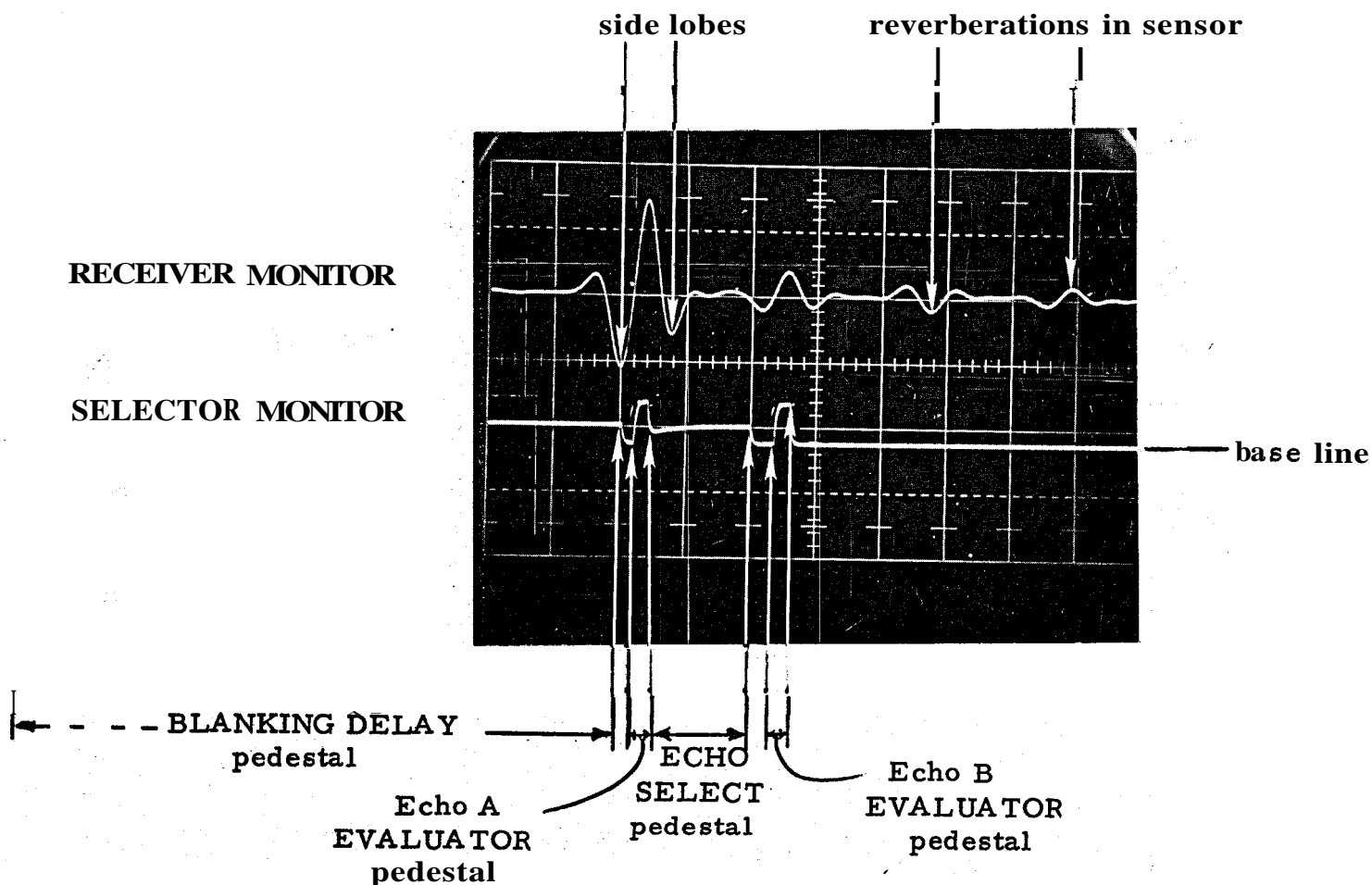
Fig. 5(b).   Upper trace (10 μ sec/cm,   5V/cm) shows room temperature multiple echoes in rhenium.   Lower trace (10 μ sec/cm, 2V/cm) shows SELECTOR MONITOR output.   This output consists of pedestals corresponding to delay flop suppression gates, and echo evaluator signals.
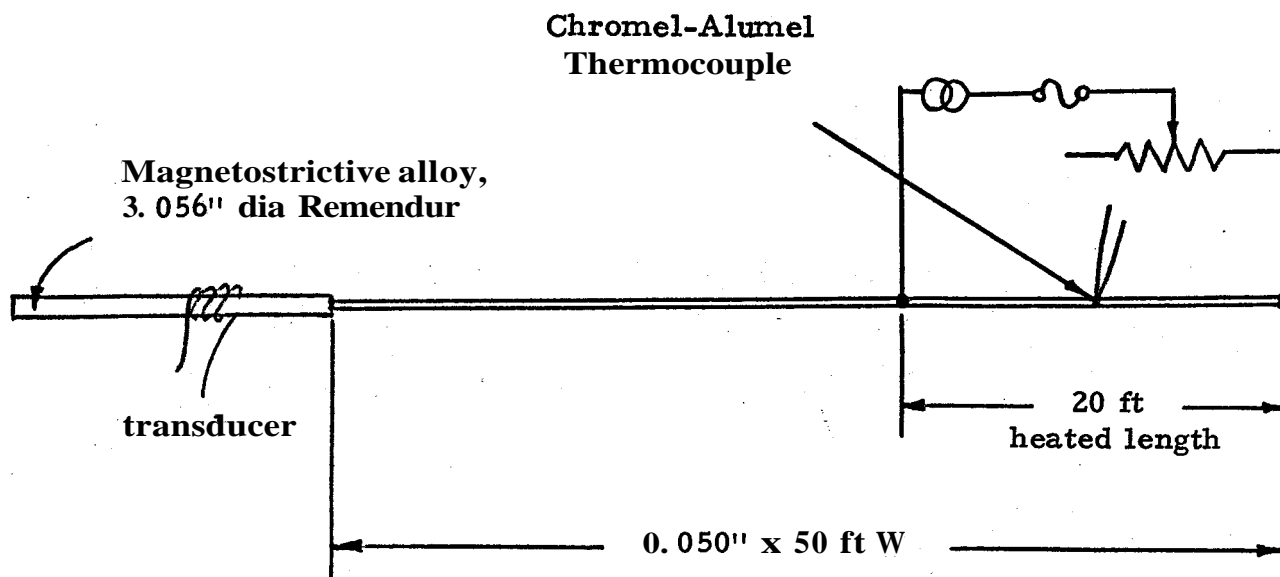
Figure 6.   Schematic diagram of ultrasonic transmission
tests on 0. 050'' x 50 ft of tungsten lead-in wire.

reflection at weld

reflection due to
wire support
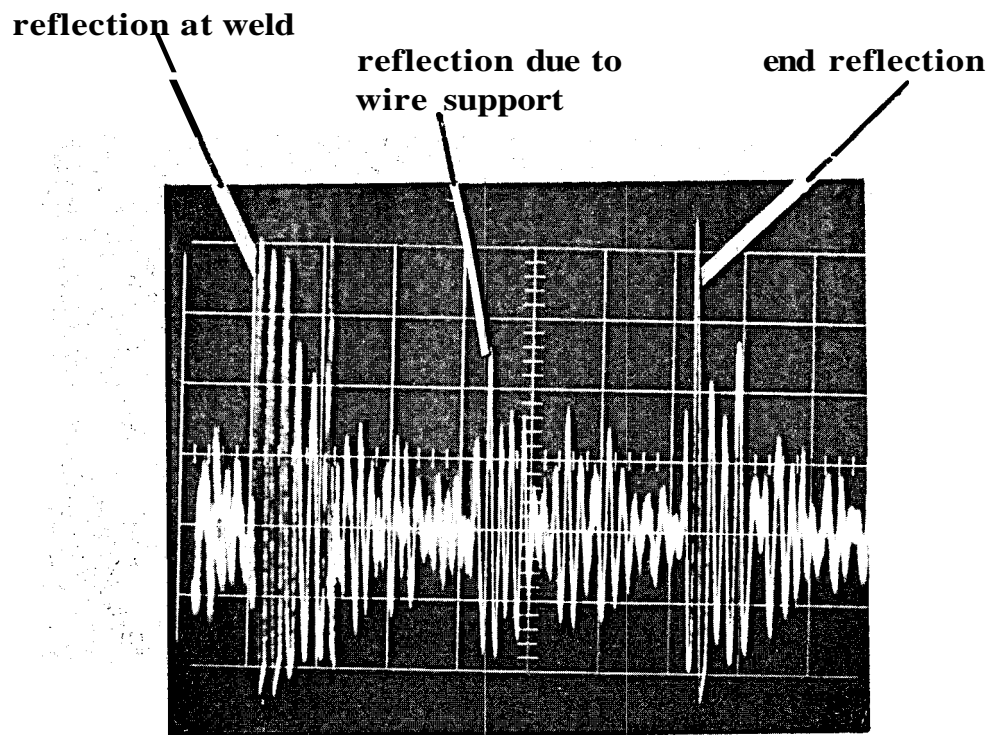
end reflection

a) Room temperature
0.2V/cm,   0.5 msec/cm

reflection at weld   end reflection
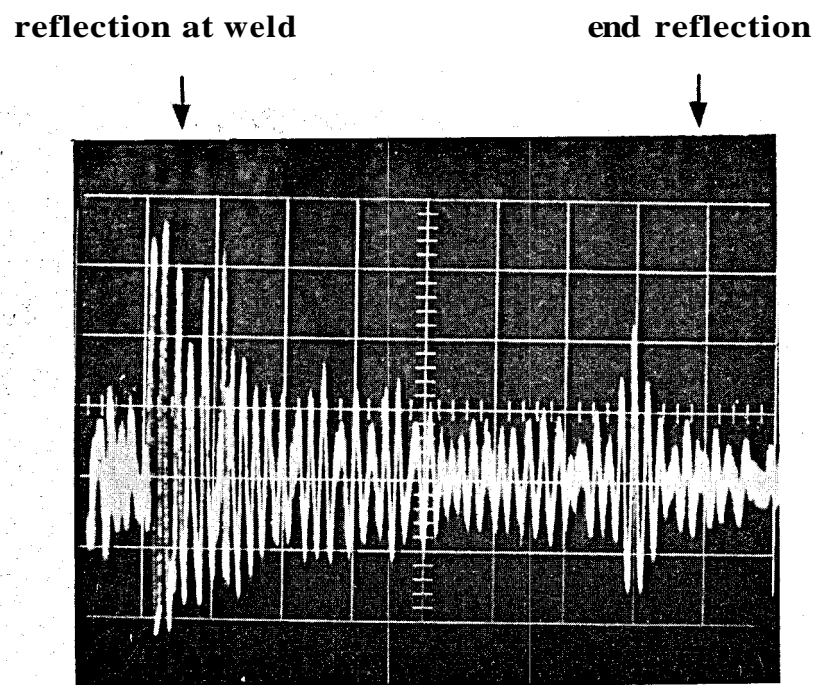
b)   2066°F - same scale.

Figure 7.   Oscilloscope displays using one 3" transmission coil
and one 3" receiver coil- 50 ft tungsten lead-in.

reflection at weld   end reflection
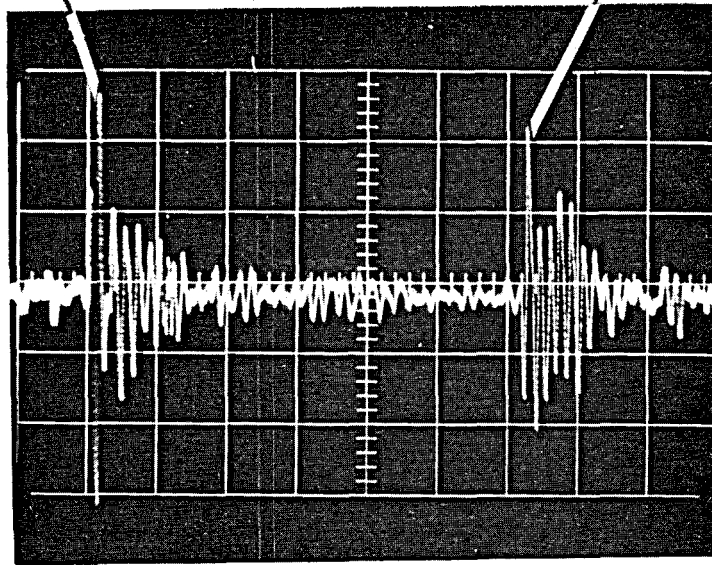
a) Room temperature

10 mV/cm, 0. 5 msec/cm
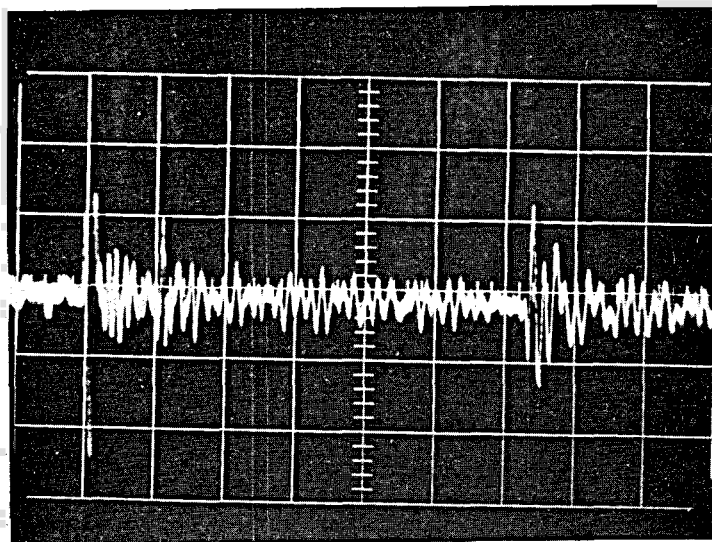
b)   1000°F - same scale.

Figure 8. Oscilloscope display using a single 3" coil for transmission and reception ‐ 50 ft tungsten lead-in.

weld

0.125" O. D. x 0. 020"w
SS 304 sheath   5" sensor

0.047" dia SS 304 wire

receive coil

transmit coil

7'6"

21' 9-1/4"
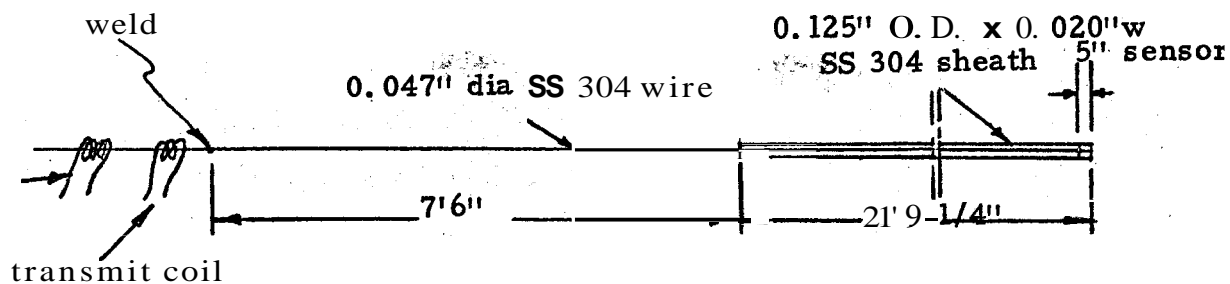
Figure 9.   Experimental set-up to determine the attenuation of
the SS 304 lead-in wire at $\sim 1250^\circ$F.

first echo   echo at end of 21 ft 4-1/4"

(a) Room temperature

0.5 msec/cm, 50 mV/cm
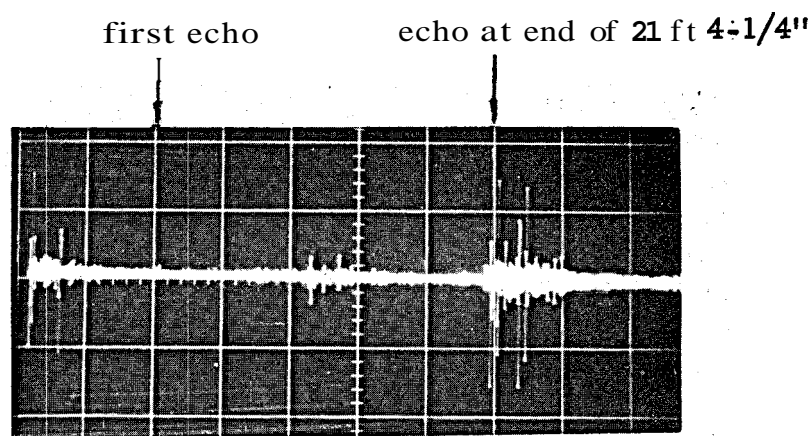
(b) At $\sim 1250^\circ$F

0.5 msec/cm, 20 mV/cm
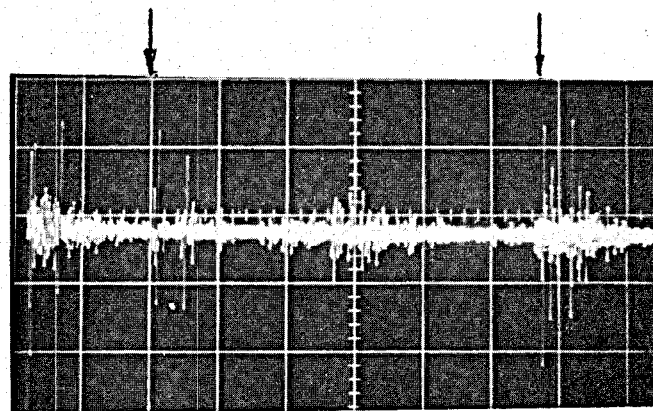
Figure 10.   Echoes from the beginning and end of a 21 ft 4-1/4" long
SS 304 lead-in wire.

Transmit
Coil

0. 067" Remendur wire

Receive
Coil

0.050" dia **x 20** ft W wire
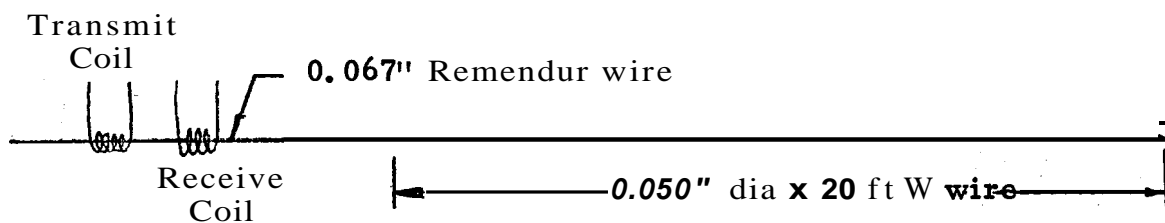
Figure 11a.   Experimental arrangement.

weld echo   end echo
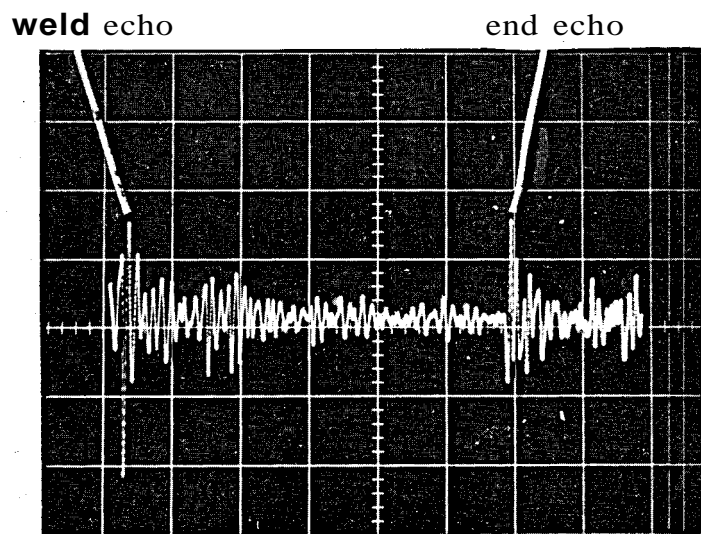
Fig. 11b.   Scope display before winding
0. **003"** spiral spacing wire;
room temperature.
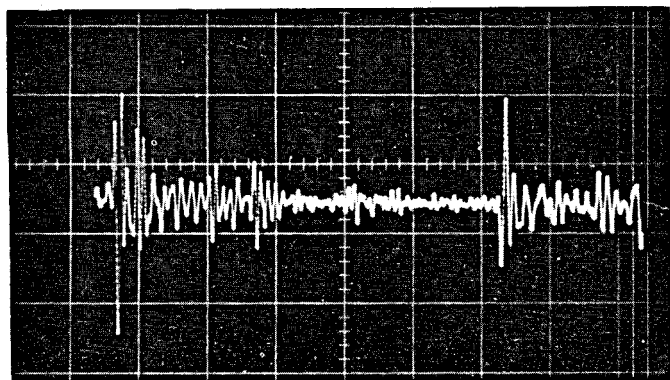
Fig. 11c.   Scope display at room tem-
perature after winding spacing
wire and sheathing in 0. **019"**
dia **x** 0. **012"** W SS **304** tube.
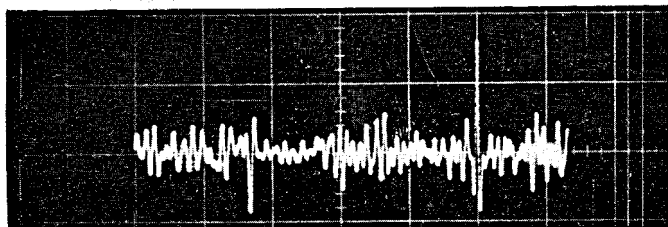
Fig. 11d.   Scope display at 1200°F;
isolated in heated SS **304** tube.

0. 5 'msec/cm   50 mV/cm

0. 056" Remendur alloy

two, 2" radius loops

20 ft of coiled 0. 050" W wire

Water (60°F)
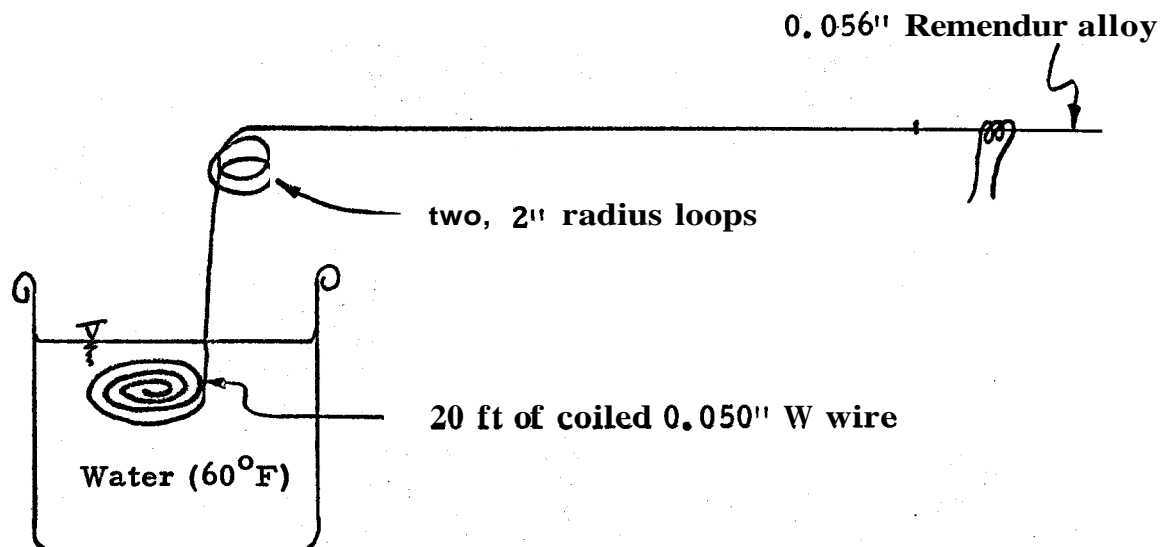
Figure 12. Schematic illustrating sodium viscosity simulation test including effect of two 2" radius loops. Test was repeated on SS 304 lead-in with same results. viz: attenuation was negligibly small.

reflection due to two
2" radius loops   end reflection
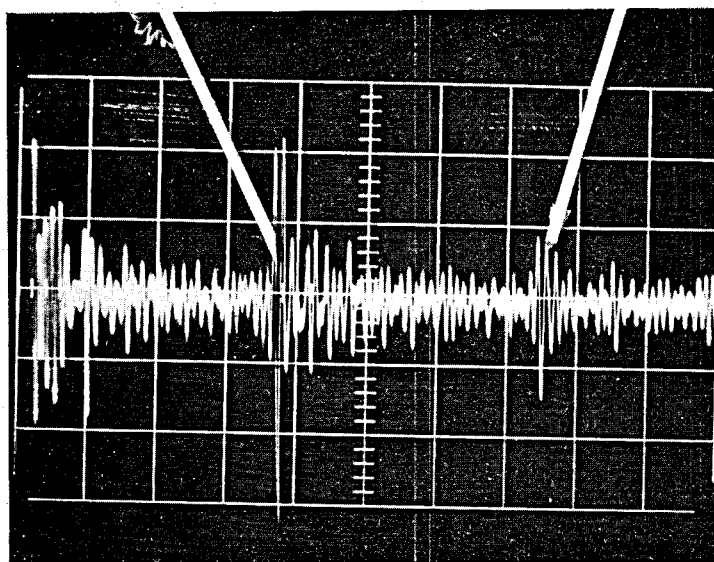
a) Before immersion in water.
    1 msec/cm, 5 mV/cm
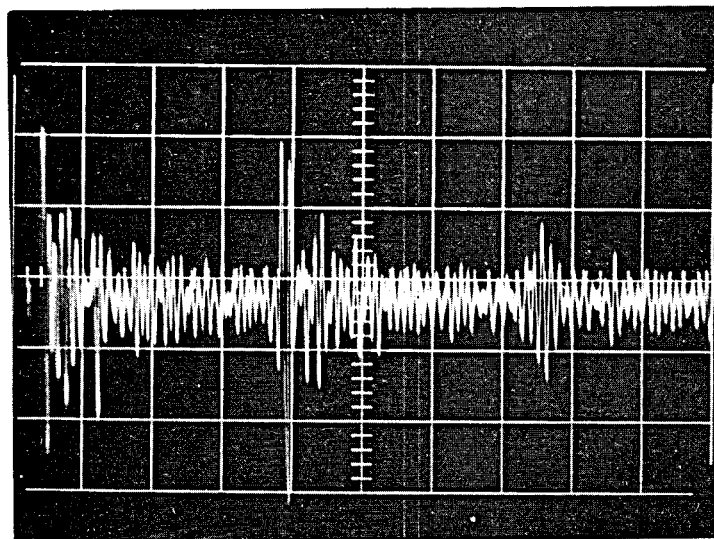
b) After immersion – same scale.

Figure 13. Effect of 2" radius loops and water – tungsten lead-in.
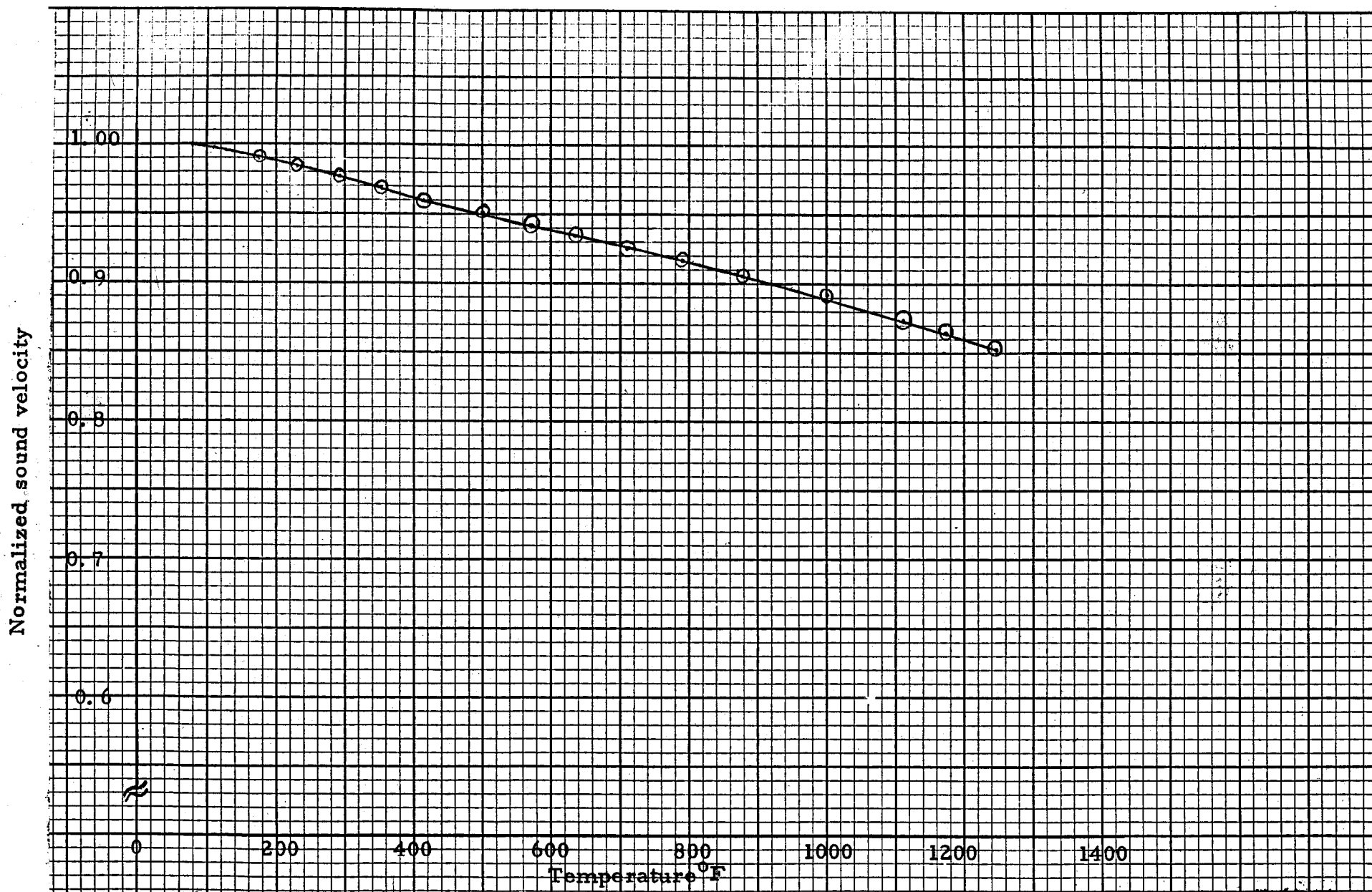
Figure 14. Normalized sound velocity in SS 304 versus temperature.
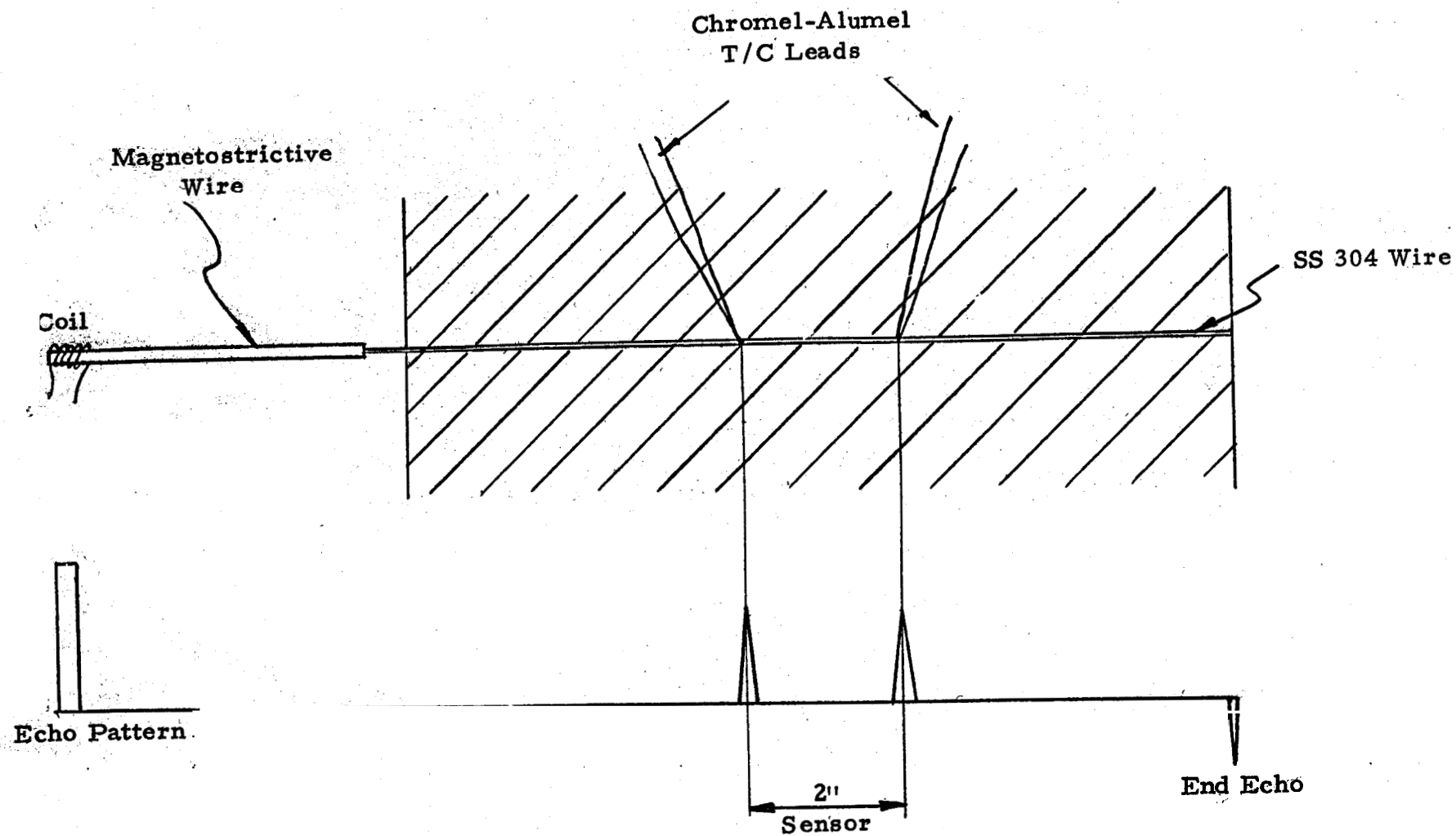
Figure 15. Schematic of oven calibration.

0. 056" Remendur Wire   Weld

.049 Spacing Wire   174 O.D. x .009 Wall Tubing

Preasse   fuel Element Tubing, Sporing Wire & Adopter

(a)

0. ~56" Remendur Wire   0.047'' Spacing Wire

Weld

174 O.D. x .009 Wall 1

(1)

Preassembled Fuel Element Tubing, Spacing Wire & Adopter

|←—6"—→|

(b)

Reflection
at (1)

End Reflection'

(c) Oscilloscope display for arrangement (b) ⁻ 1V/cm, 20 μ sec/cm
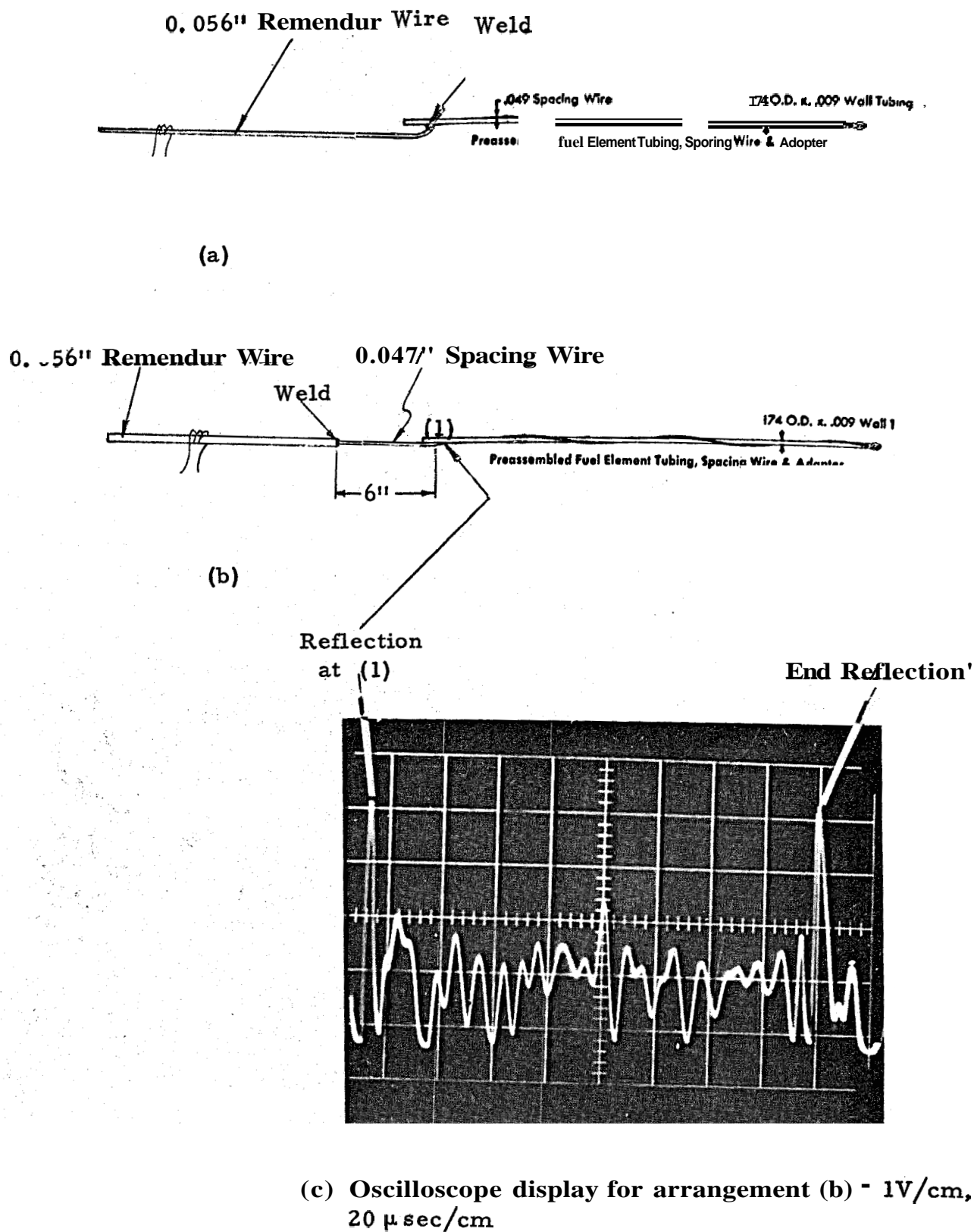
Figure 16. Experimental arrangements illustrating the use of the spacing wire as temperature sensor.

0. 056" Remendur Wire

Weld

.049 Spacing Wire

.174 O.D. x .009 Wall Tubing

(a)

Preassembled Fuel Element Tubing, Spacing Wire & Adapter (b)

(a)

reflection from (a)   end echo from (b)
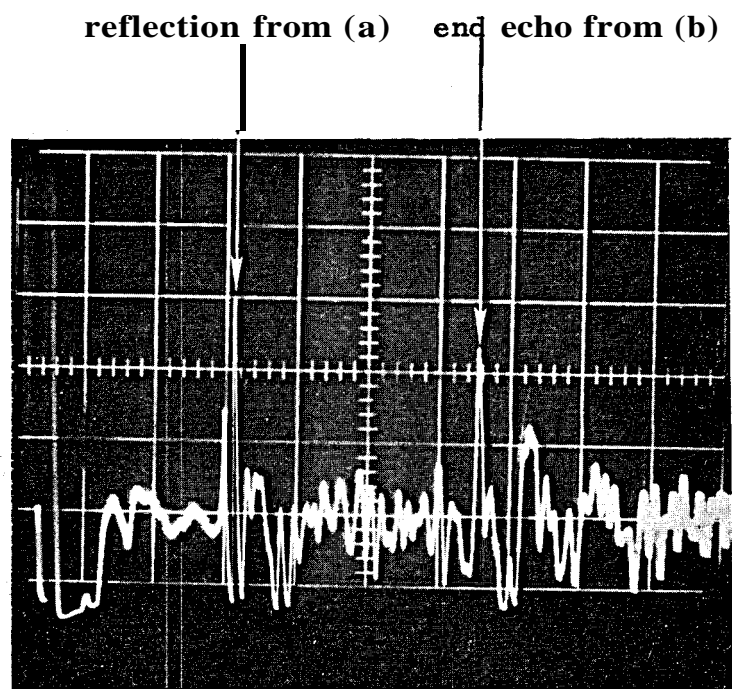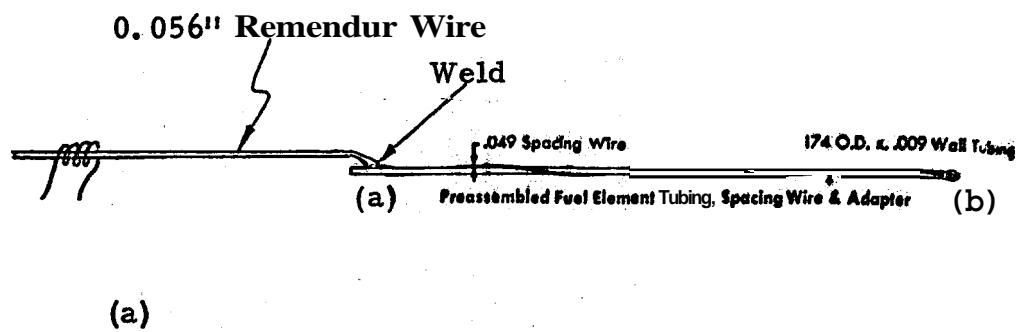
(b) Oscilloscope display - 1V/cm, 50 μ sec/cm

Figure 17,   Experimental arrangement illustrating the use of the .cladding
as temperature sensor.

Transducer

Magnetostrictive
wire

Weld

Lead-in wire

Needle valve

Bellows valve

Plug
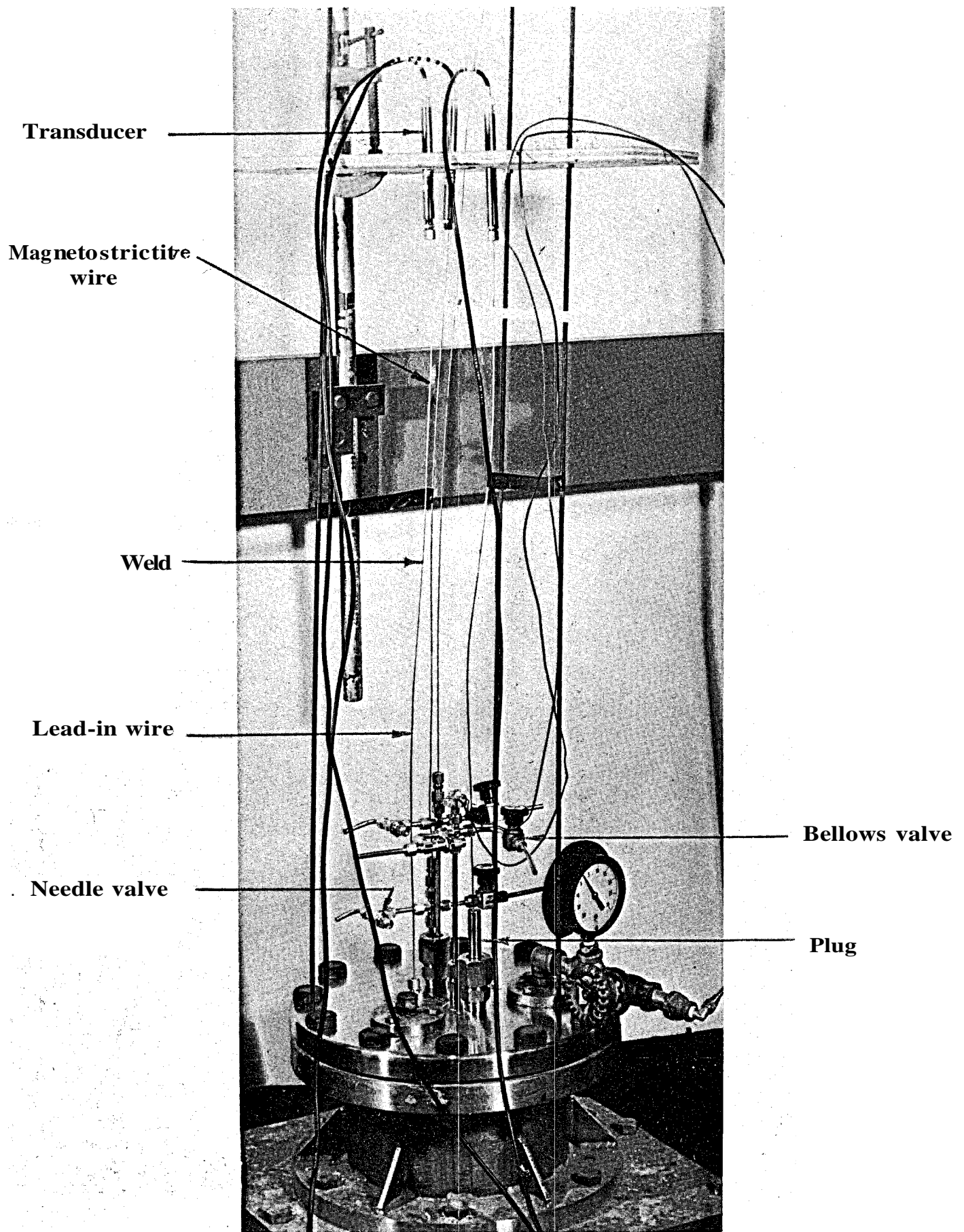
Figure 18. Overall view of flange assembly.
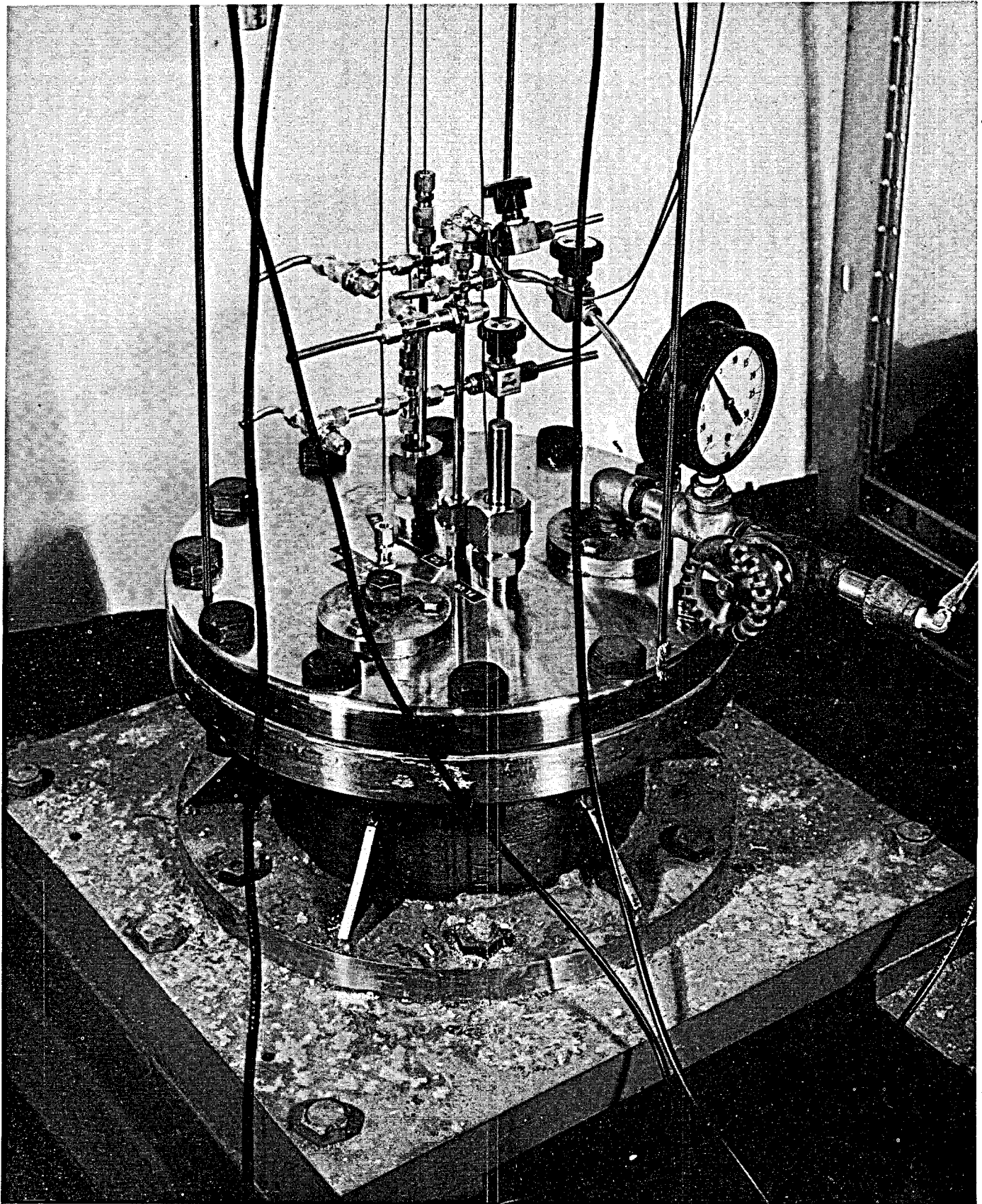
Figure 19. Top view of flange assembly – closeup.

Figure 20. Sketch of probe cluster for tests in sodium at Argonne National Laboratory.
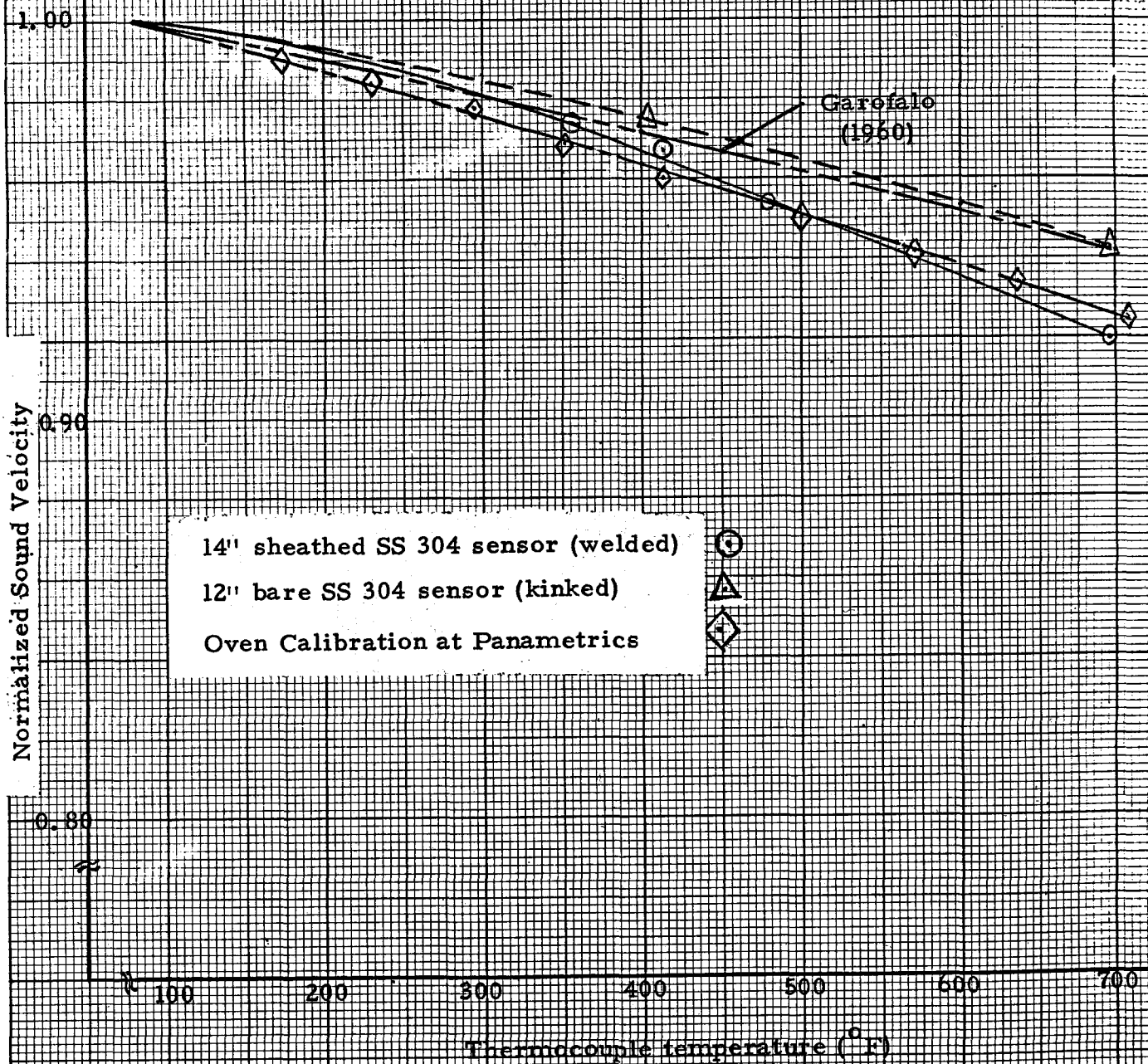
Figure 21. Sound velocity vs. thermocouple temperature.
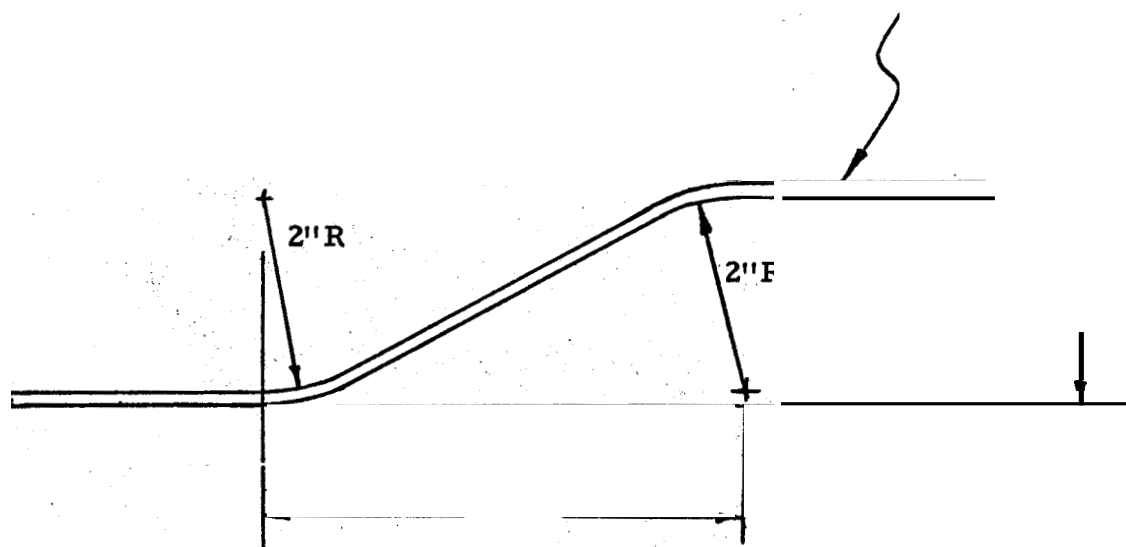
Figure 22. **S-shaped curve in sheath and lead-in wire.**

1/8" O D x 0.020" Wall
x 20 ft SS304 Sheath

Conax

100 psi

Gas Bottle

2"R

2"R

A. C. heated to ~1060°F

Conax

Pressure Tight
Transducer Assembly.

PANATHERM
5010

Electrical
Leads

D C
Heated to
~ 5000°F

0.062" O D x 0.004"W x 6"Ta tube
containing 1.5" Re sensor

Evacuated
6" Glass Cross
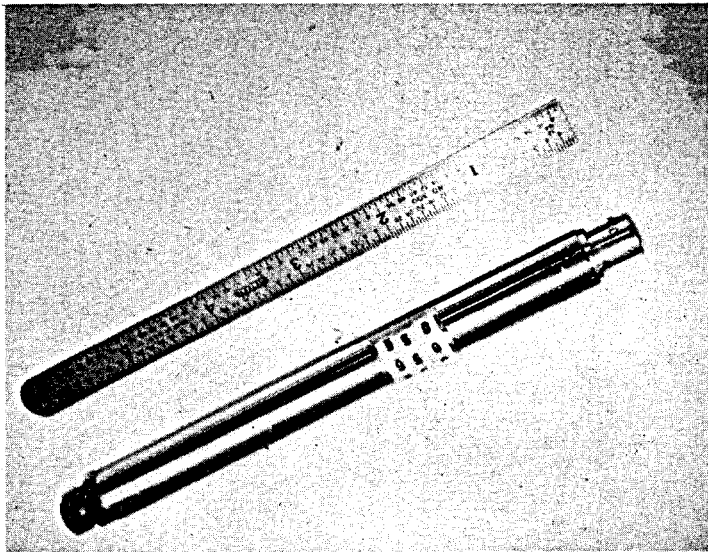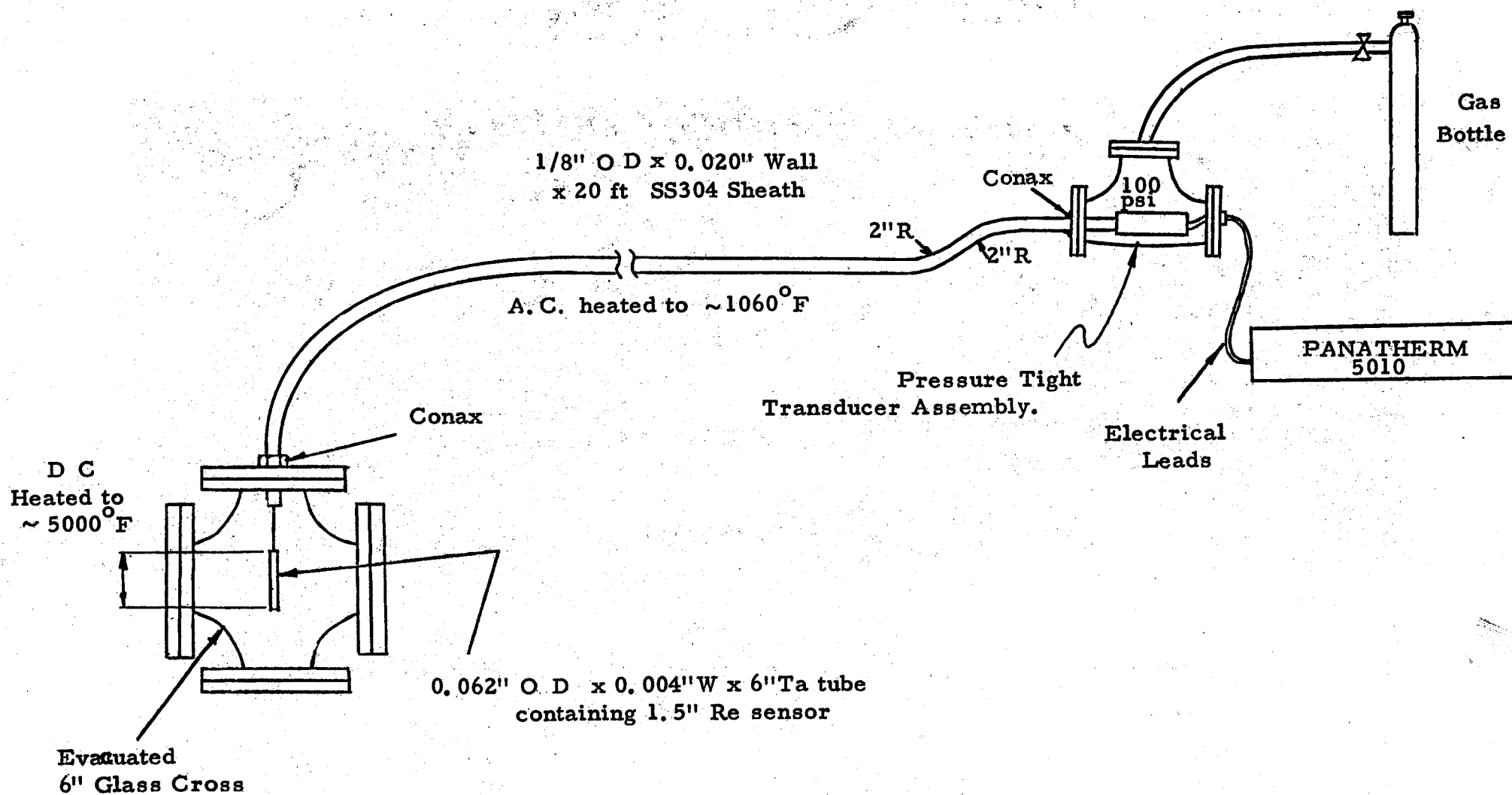
Figure 24. Schematic of system test.
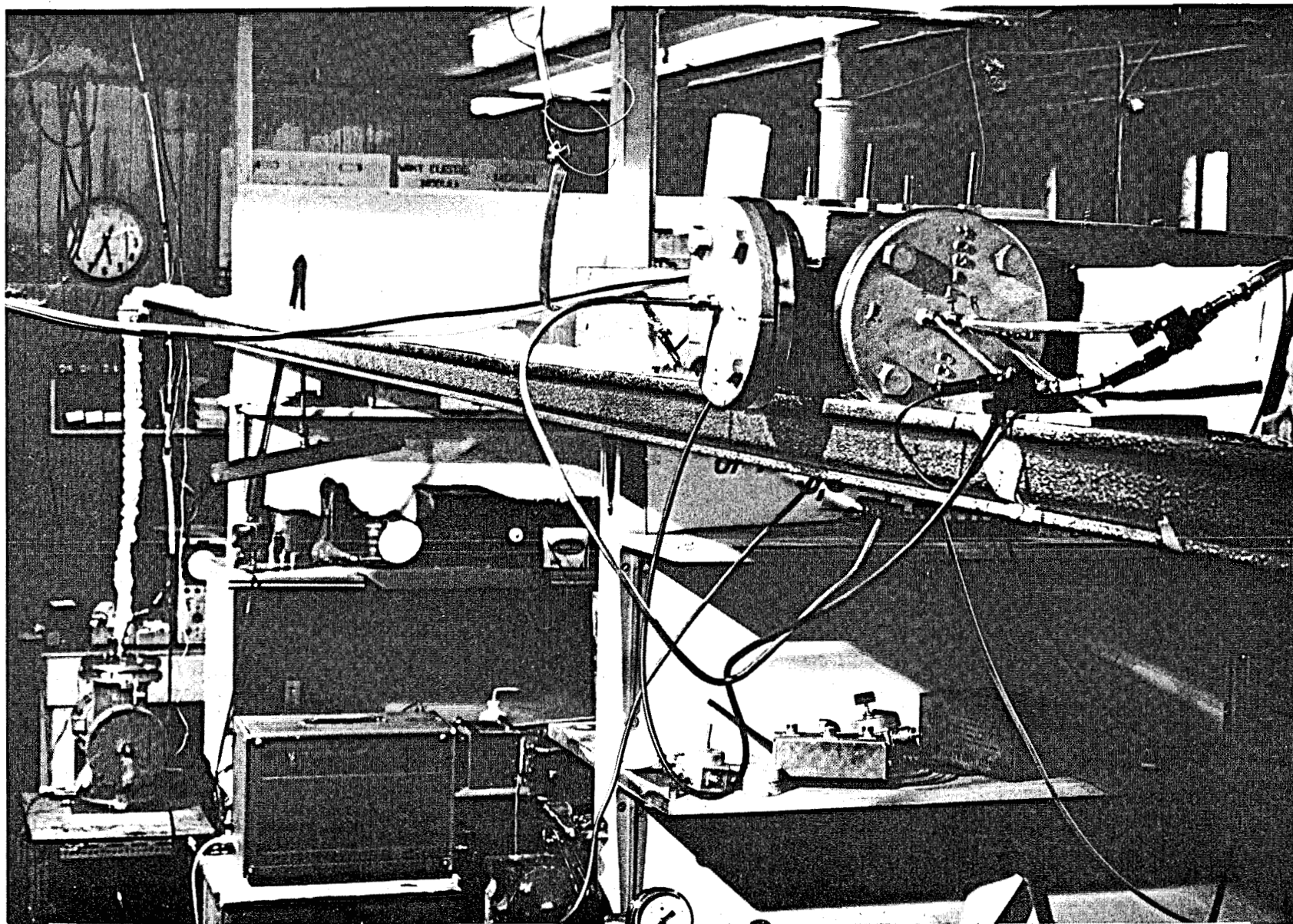
Figure 25. General view of ultrasonic line showing pressure tight transducer, 20 ft sheathed lead-in containing two bends with 2 in. radius of curvature, and high temperature chamber in which Re sensor is heated to 5000°F.
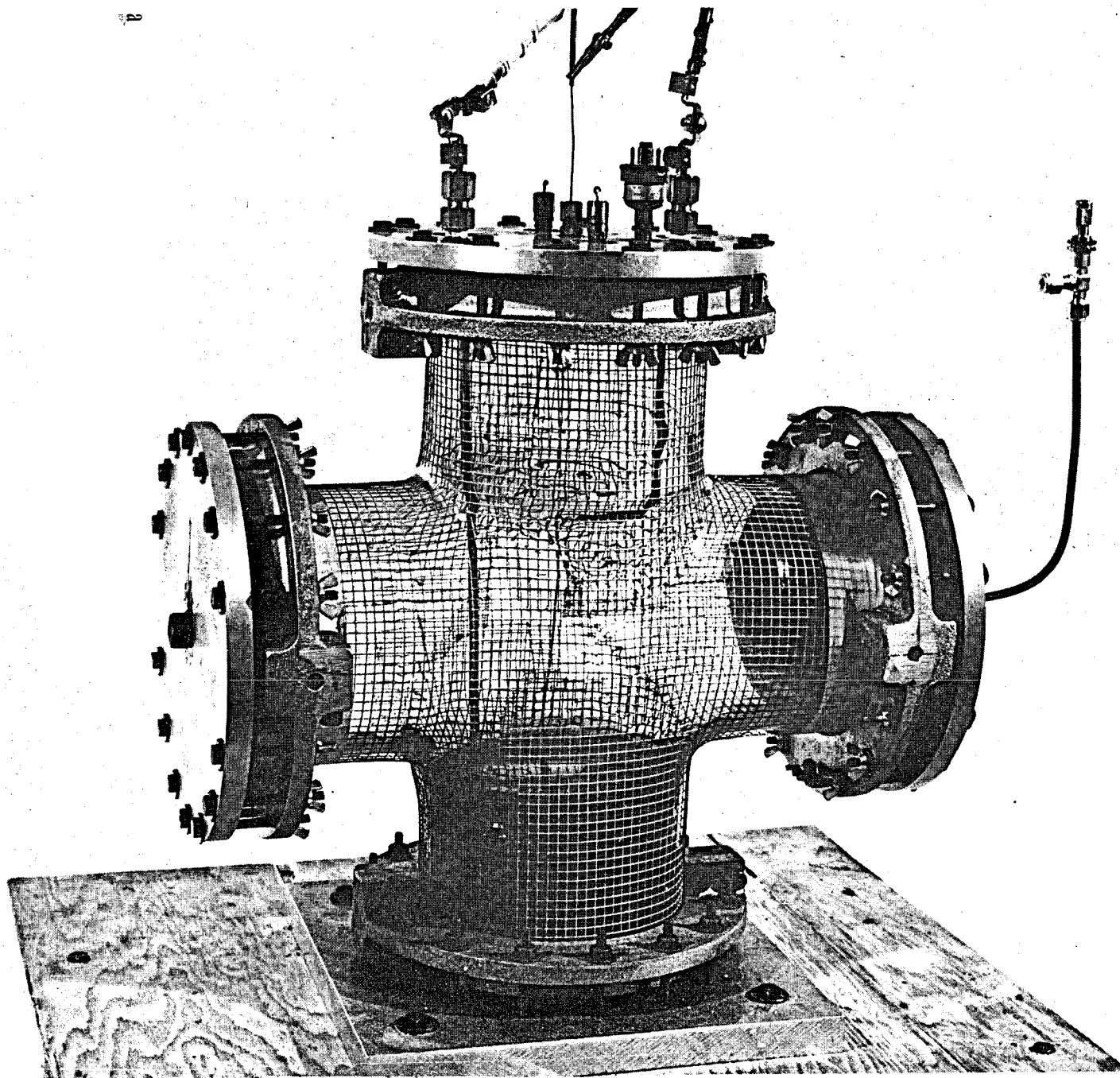
Figure Z6   Close-up of 5000°F chamber

0.056" dia magnetostrictive
wire

0.047" dia x 30' SS 304

0.047"dia x 1' SS 304
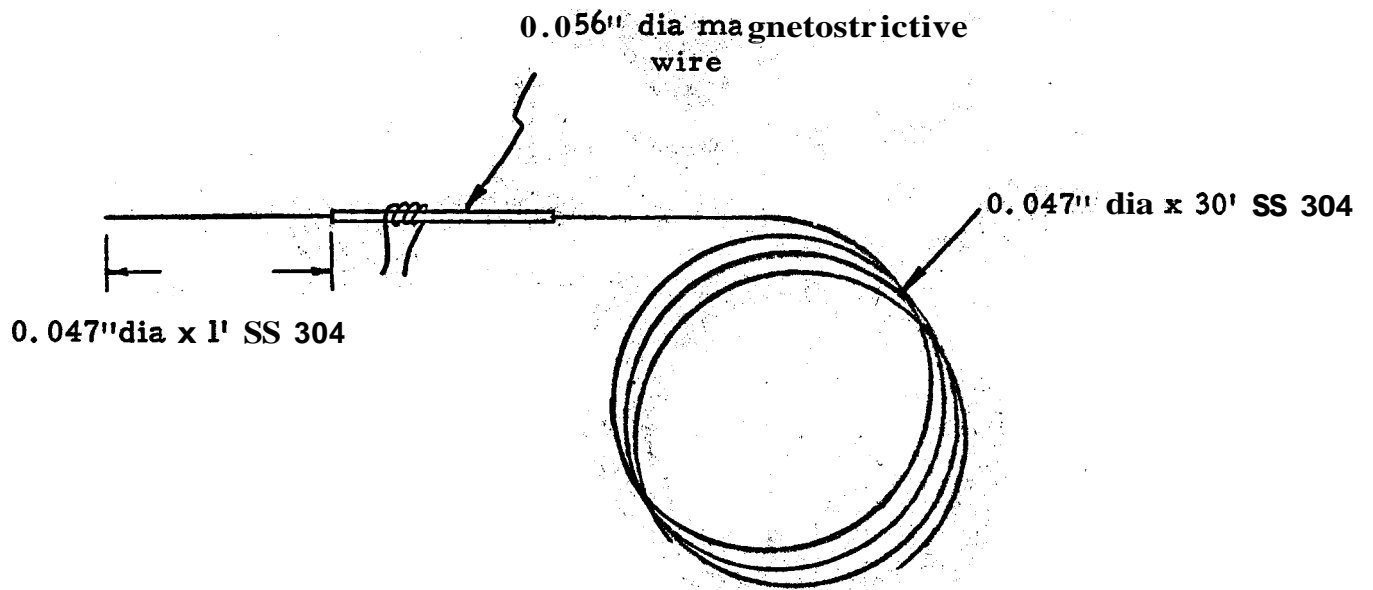
Figure 27. Experiment to determine room temperature
attenuation in SS 304.
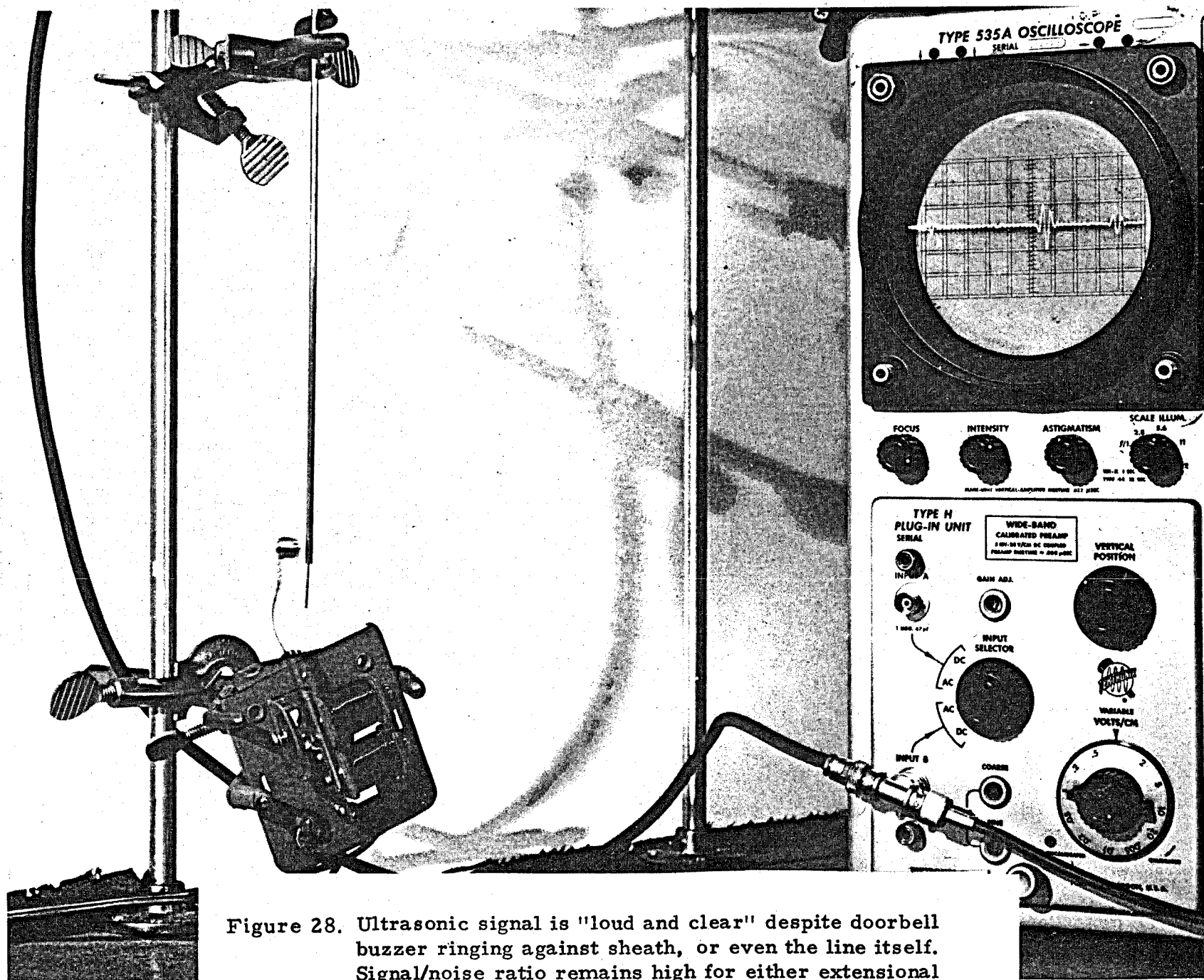
Figure 28. Ultrasonic signal is "loud and clear" despite doorbell
buzzer ringing against sheath, or even the line itself.
Signal/noise ratio remains high for either extensional
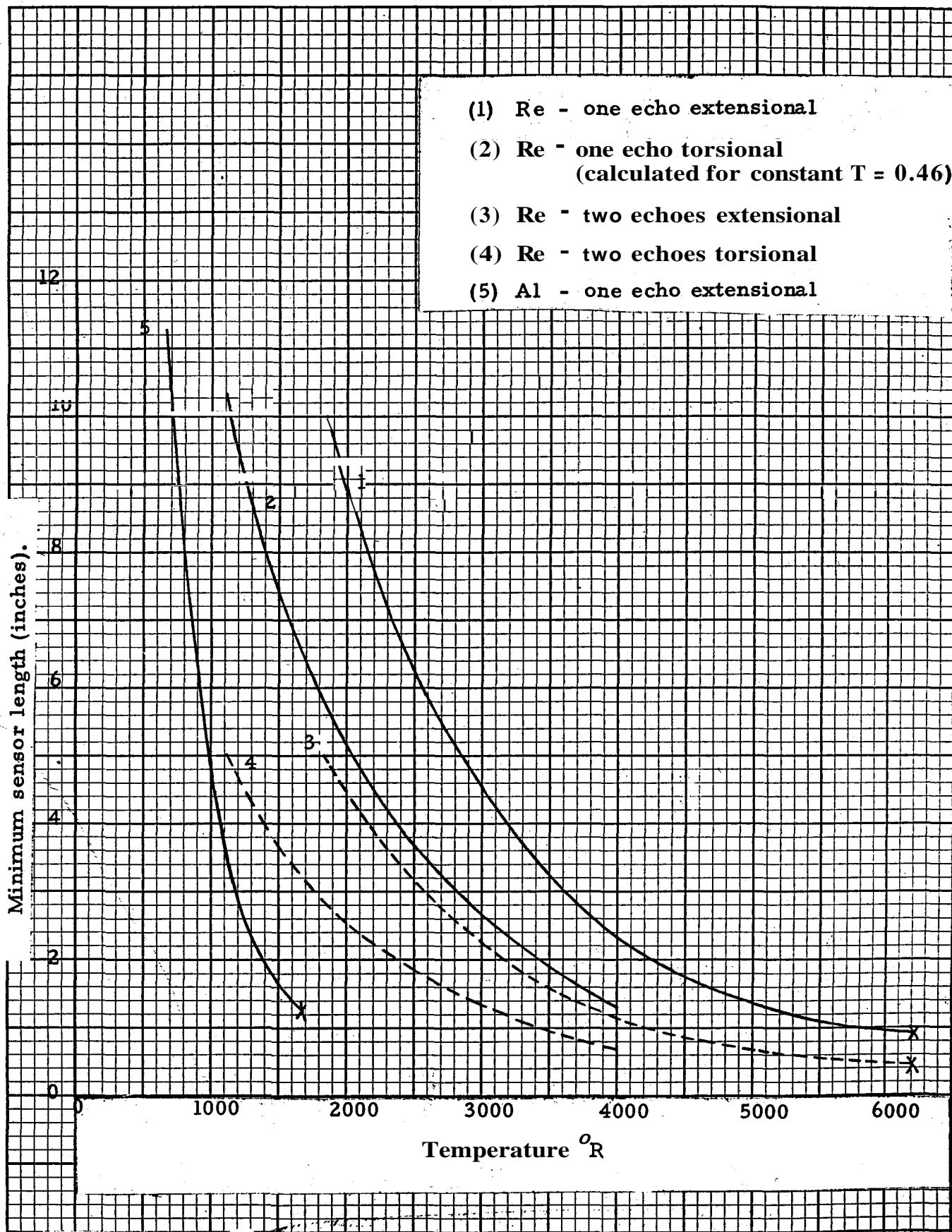or torsional waves.

(1) Re - one echo extensional

(2) Re - one echo torsional
    (calculated for constant T = 0.46)

(3) Re - two echoes extensional

(4) Re - two echoes torsional

(5) Al - one echo extensional

Figure 29.   Minimum sensor length for a temperature sensitivity of
± 1% and a time measurement uncertainty of ± 0.1 μsec.
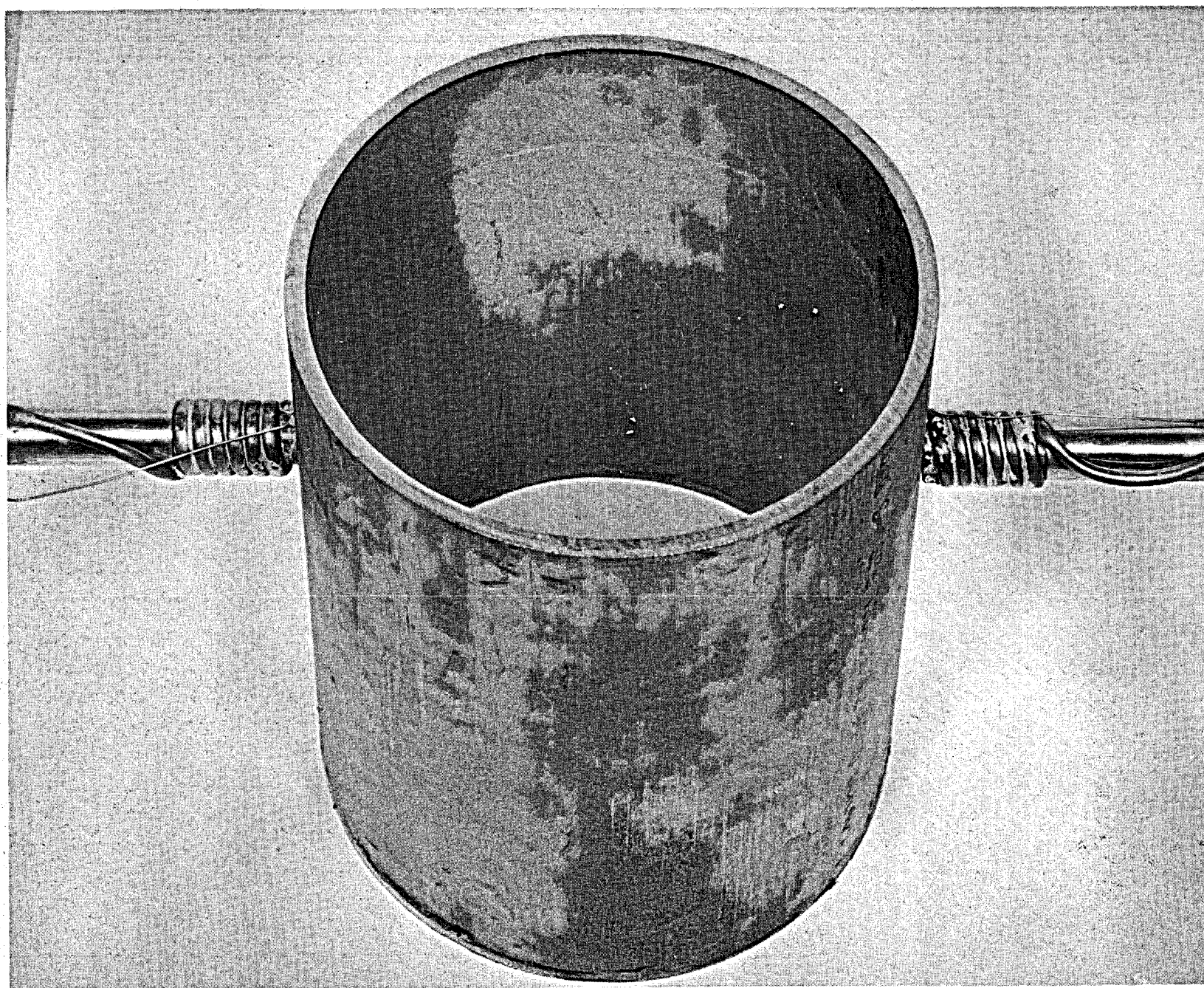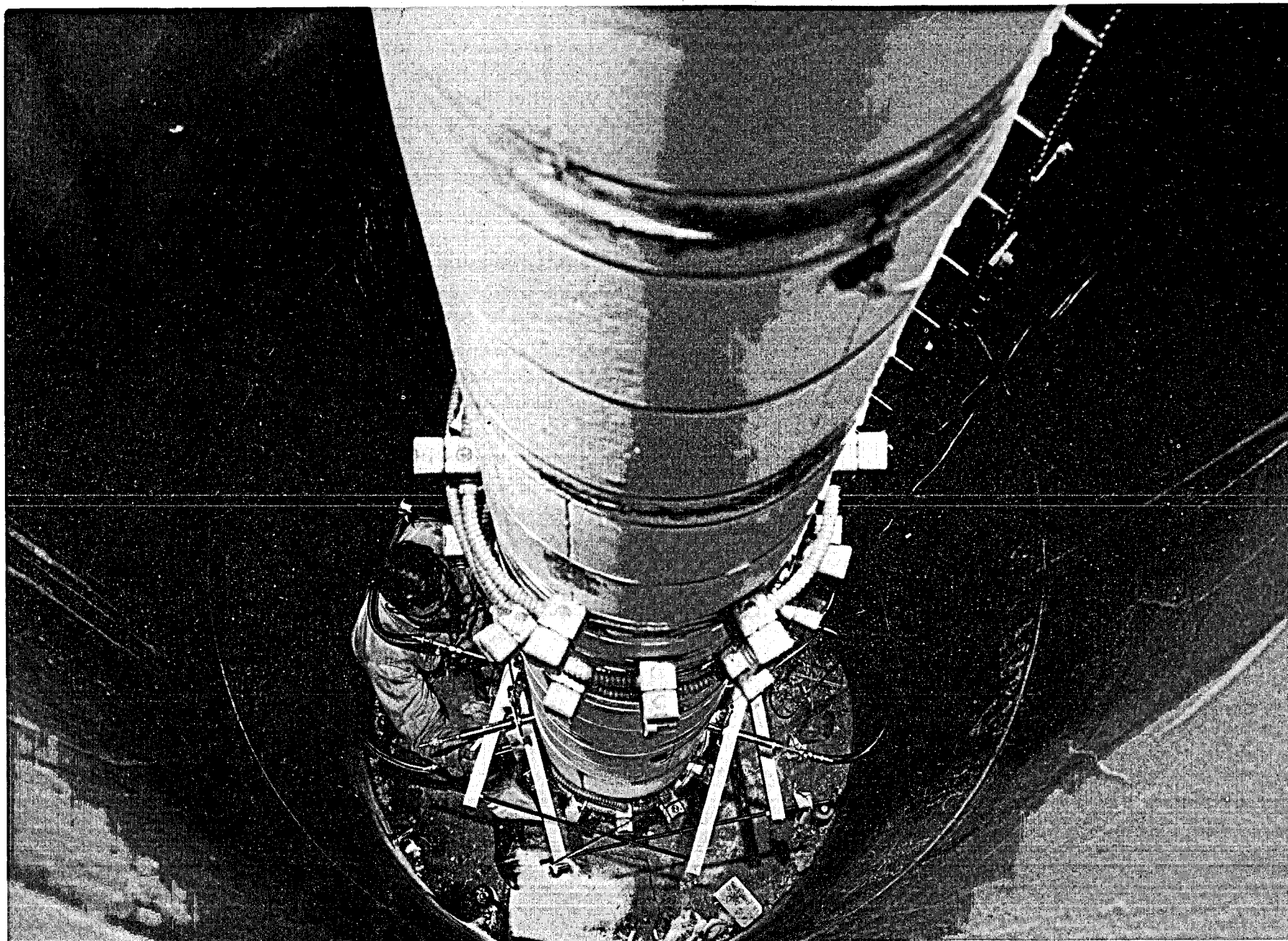
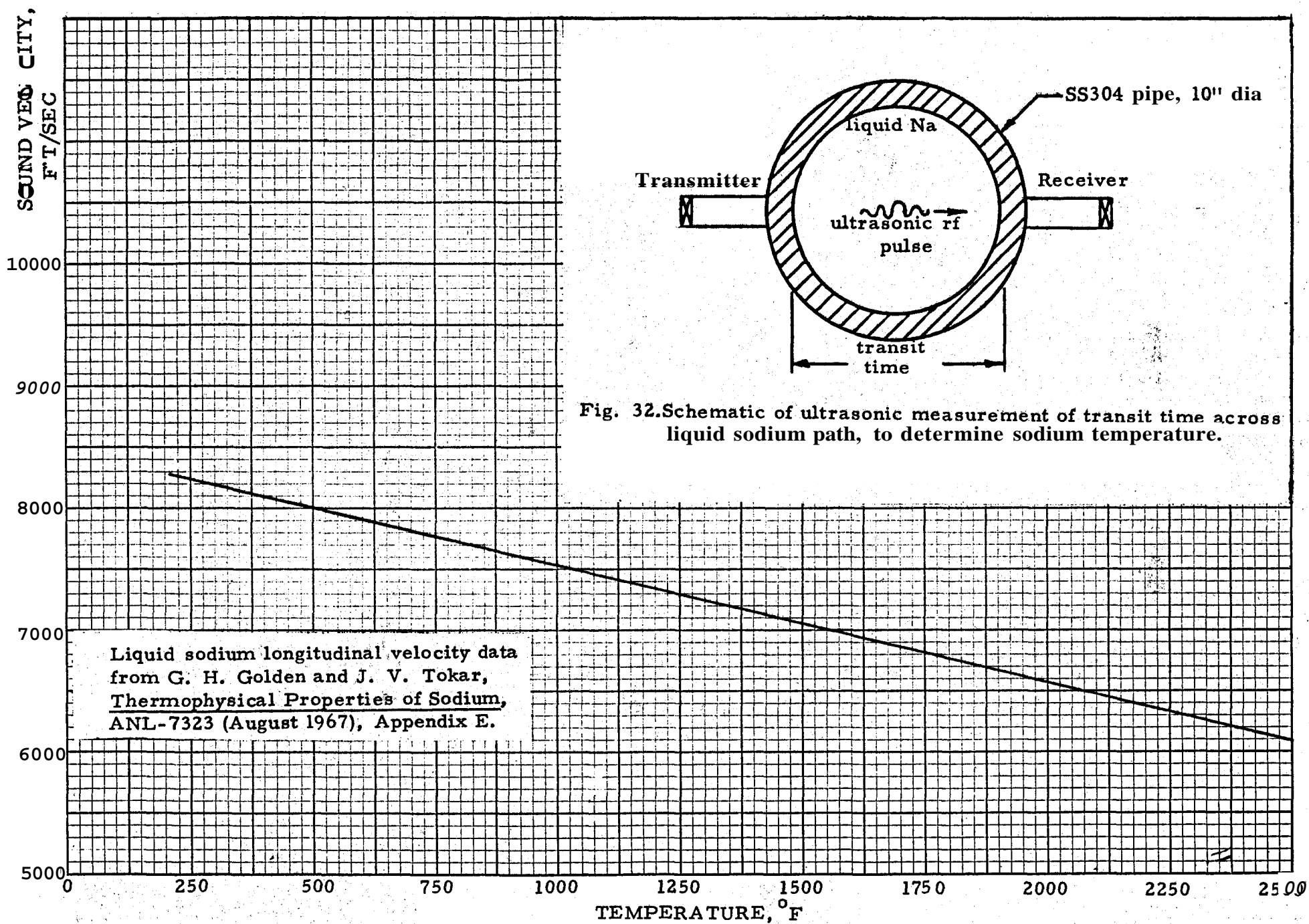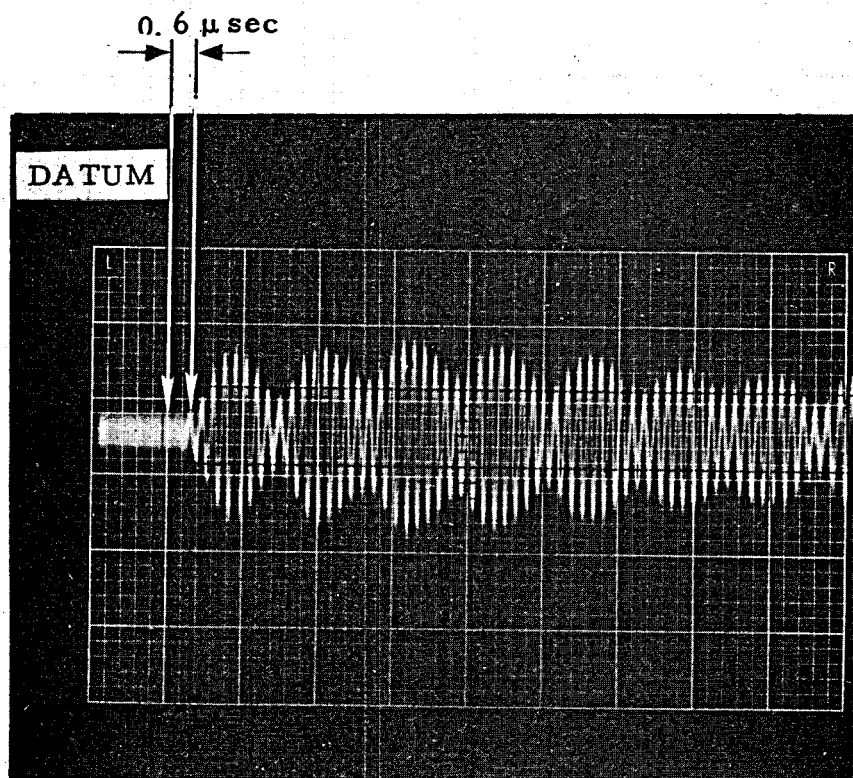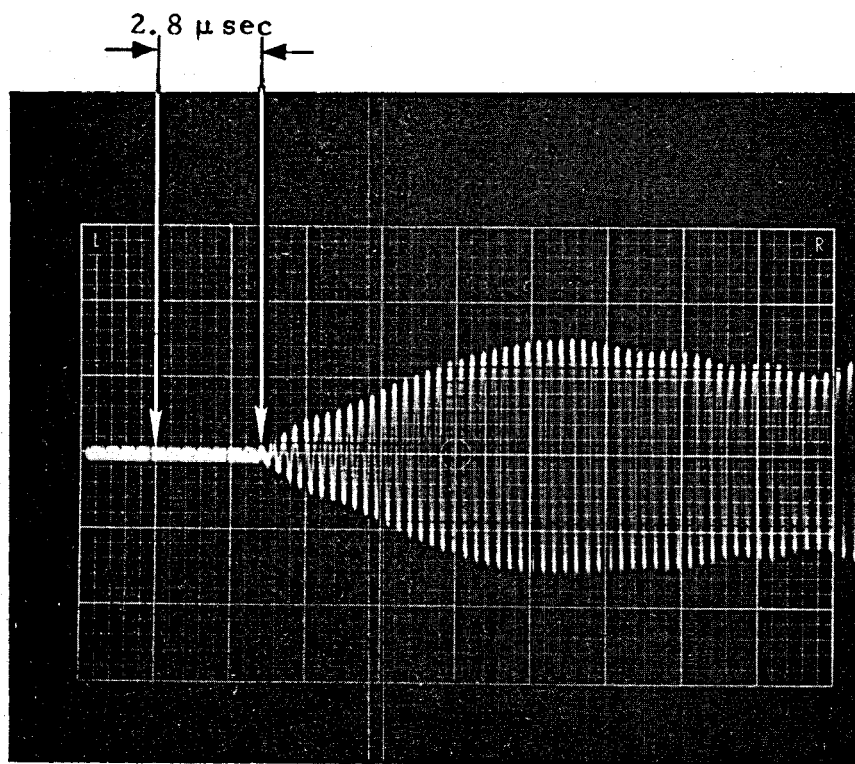Fig. 30. Longitudinal probe configuration.

Figure 31. On-site arrangement of longitudinal and shear probes to ultrasonically
determine the liquid sodium temperature. ANL oscillator rod facility
May 2nd, 1968.

Fig. 32. Schematic of ultrasonic measurement of transit time across liquid sodium path, to determine sodium temperature.

Liquid sodium longitudinal velocity data from G. H. Golden and J. V. Tokar, Thermophysical Properties of Sodium, ANL-7323 (August 1967), Appendix E.

Longitudinal wave transit time. 0. 6 μ sec shift from datum, 543°F,
2 μ sec/cm, 0. 1 V/cm

2.8 psec shift, 688°F, 2 μ sec/cm, 0.1 V/cm
Relative shift of 2.2 μ sec is due to ΔT = 688-543 = 145°F

Figure 33. Longitudinal wave transmission through liauid sodium

FIG.34

Block diagram.